QUARTERLY OF APPLIED MATHEMATICS
VOLUME LXXI, NUMBER 4
DECEMBER 2013, PAGES 729–753
S 0033-569X(2013)01308-7
Article electronically published on August 29, 2013

BIFURCATION OF HEMITROPIC ELASTIC RODS UNDER AXIAL THRUST

By

TIMOTHY J. HEALEY (*Department of Mathematics and Department of Mechanical & Aerospace Engineering, Cornell University, Ithaca, New York*)

AND

CHRISTOPHER M. PAPADOPOULOS (*Department of Engineering Science and Materials, University of Puerto Rico, Mayagüez, Puerto Rico*)

Abstract. In this work we consider the analysis of unshearable, hemitropic hyperelastic rods under end thrust alone. Roughly speaking, a nominally straight hemitropic rod is rotationally invariant about its centerline but lacks the reflection symmetries characterizing isotropic rods. Consequently a constitutive coupling between extension and twist is natural. We provide a rigorous bifurcation analysis for such structures under "hard" axial loading. First, we show that the initial post-buckling behavior depends crucially upon the boundary conditions: if both ends are clamped against rotation, the initial buckled shape is spatial (nonplanar); if at least one end is unrestrained against rotation, the buckled rod is twisted but the centerline is planar. Second, we show that as with isotropic rods, nontrivial equilibria of hemitropic rods occur in discrete modes, but unlike the isotropic case, such equilibria need not be compressive but could also be tensile. Finally, we prove an exchange of stability between the trivial line of solutions and "mode 1" bifurcating branches in accordance with the usual theory.

1. Introduction. Long slender structures often exhibit an orientation or handedness in their natural relaxed states. Examples include biological filaments like idealized DNA molecules and man-made objects like cables. Accordingly, a good mechanical model of such structures should capture handedness or chirality. The simplest such model, viz., a *hemitropic* rod, was proposed in [7]. Roughly speaking, a nominally straight, hemitropic rod is rotationally invariant about its centerline but does not generally possess the reflection symmetries characterizing isotropic rods. Hemitropy can be rigorously obtained by starting with the class of rods having the symmetry of a regular cylindrical helix and then taking the limit as the pitch goes to zero; cf. [8].

Received December 14, 2011.
2010 *Mathematics Subject Classification.* Primary 74K10, 74G60; Secondary 74B20, 37G40.
Key words and phrases. Hemitropy, Cosserat rod, symmetry, bifurcation.
E-mail address: tjh10@cornell.edu
E-mail address: christopher.papadopoulos@upr.edu

In this work we consider the analysis of unshearable, hyperelastic hemitropic rods under end thrust alone. What arises naturally here as the distinguishing feature is a constitutive coupling between extension and twist. This phenomenon is well known in the behavior of both wire rope [4] and long DNA molecules [13], and in each case simple quadratic stored energy functions have been proposed. Here we give a rigorous bifurcation analysis for such structures under "hard" axial loading. In particular, we show that the behavior of the initial post-buckled configuration depends crucially upon the boundary conditions: *clamped* rods (both ends restrained against end rotation) have nonplanar, initial post-buckled configurations, while *unclamped* rods (i.e., those in which at least one end rotation is unconstrained) always buckle in such a way that the centerline lies in a plane.

Of course the buckling and post-buckling analysis of straight elastic rods subject to end thrust dates back to the seminal work of Euler [5]. The literature on such problems since that time is immense, and we make no attempt to account for it here. However, we note that (to the best of our knowledge) the buckling and post-buckling analysis of chiral elastic rods is absent from the literature.

The outline of this work is as follows: In Section 2 we summarize the basic field equations for hyperelastic rods, providing the definition of hemitropy and its subsequent representation. In Section 3 we analyze a straight hemitropic rod under dead-load thrust with fixed-free boundary conditions, i.e., one end totally clamped with the opposing, loaded end unconstrained. Our approach here is completely classical. Exploiting hemitropy, we introduce a semi-convected basis field, much like in the analysis of the Lagrange top [16]. We then readily demonstrate that all equilibria of the rod are characterized by a planar centerline, generally accompanied by nonzero twist.

In Sections 4-6, which form the heart of the paper, we treat fixed-fixed hemitropic rods subject to "hard-load" axial displacements at the ends. We employ a coordinate-free approach and use modern bifurcation theory to study the initial post-buckling behavior, which is completely distinct from that of fixed-free rods. In particular, we show that the initial post-buckled shape is spatial (nonplanar). This is also in stark contrast to the planar initial post-buckling of isotropic rods under pure end thrust. We identify and exploit the $O(2) \subset SO(3)$ symmetry inherent in the problem, which is necessary to carry out the rigorous bifurcation analysis in Sections 4 and 5. We further conclude that all local bifurcations are "pitchforks". In Section 6 we examine the exchange of stability - via minimum potential energy criterion - along the trivial (straight) solutions as the loading parameter passes though the "first" critical value. Due to the presence of constraints, the formulation here is not standard. Motivated by [12], we introduce appropriate projection operators to identify an equivalent unconstrained eigenvalue problem that plays a crucial role in the analysis of the second variation of the governing energy functional. We demonstrate that solutions are stable for loading parameters below the first critical value.

2. General formulation. Throughout this work we denote *vectors* (elements of $\mathbb{E}^3$, which denotes the tangent space of 3-dimensional Euclidean point space) by boldface, lowercase symbols, *e.g.* $\mathbf{a}, \mathbf{x}$, etc. Linear transformations of $\mathbb{E}^3$ into itself are denoted by boldface, uppercase symbols, *e.g.* $\mathbf{A}, \mathbf{T}$, etc.

Let $\{\mathbf{e}_1, \mathbf{e}_2, \mathbf{e}_3\}$ denote a standard right-handed, orthonormal basis for $\mathbb{E}^3$. We consider a Special Cosserat rod that occupies a straight, stress-free reference configuration $\{s\mathbf{e}_3 : s \in [-\frac{1}{2}, \frac{1}{2}]\}$. Let $\mathbf{r}(s) \in \mathbb{E}^3$ denote the position vector (with respect to some fixed origin) of the material point originally located at s in the reference configuration. We let $\mathbf{R}(s) \in SO(3)$ denote the rotation of the cross-section originally located at s and spanned by $\{\mathbf{e}_1, \mathbf{e}_2\}$. Three unit-vector fields of an orthonormal frame field, called *directors*, are defined by

$$\mathbf{d}_i(s) \;=\; \mathbf{R}(s)\mathbf{e}_i, \quad i \;=\; 1, 2, 3, \tag{2.1}$$

and are used in the Special Cosserat theory to quantify the *orientation* of each cross section in the deformed configuration. The deformed configuration of the rod is thus uniquely specified by the fields $\mathbf{r}(s)$ and $\mathbf{R}(s)$ on $[-\frac{1}{2}, \frac{1}{2}]$, as shown in Figure 1.

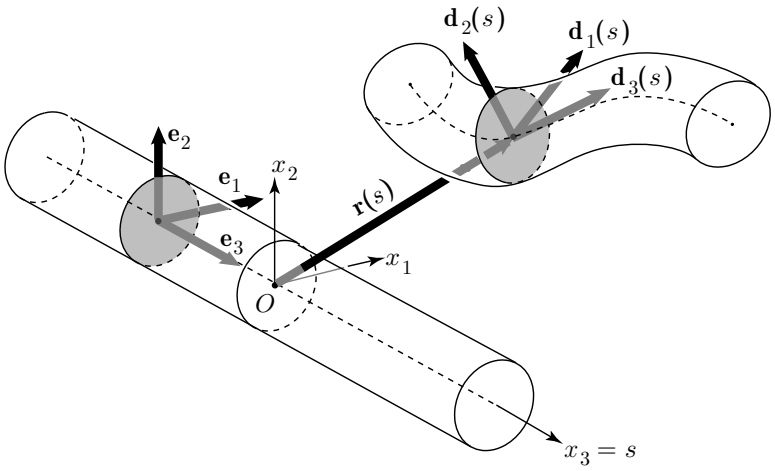

FIG. 1. Kinematics of the Special Cosserat rod

Differentiation of (2.1) yields

$$\mathbf{d}_i'(s) \;=\; \mathbf{R}'(s)\mathbf{R}^T(s)\mathbf{d}_i(s), \quad i = 1, 2, 3. \tag{2.2}$$

Since the tensor field $\mathbf{R}'\mathbf{R}^T$ is skew-symmetric, there is a vector field $\boldsymbol{\kappa}$ such that

$$\mathbf{d}_i'(s) \;=\; \boldsymbol{\kappa}(s) \times \mathbf{d}_i(s), \quad i \;=\; 1, 2, 3. \tag{2.3}$$

We then express $\mathbf{r}'$ and $\boldsymbol{\kappa}$ in terms of *convected* coordinates ν_i and κ_i, respectively, as follows:

$$\mathbf{r}' \;=\; \nu_i \mathbf{d}_i \quad \text{and} \quad \boldsymbol{\kappa} \;=\; \kappa_i \mathbf{d}_i, \tag{2.4}$$

where we employ the usual summation convention that repeated Latin indices imply summation from 1 to 3.

We require each configuration of the rod to satisfy the nonpenetration condition

$$\nu_3 \;=\; \mathbf{d}_3 \cdot \mathbf{r}' \;> 0. \tag{2.5}$$

We let $\mathbf{n}(s)$ and $\mathbf{m}(s)$ denote the internal contact force and internal contact couple, respectively, acting on the cross-section originally at s in the reference configuration. In

the absence of body forces and body couples, the well-known local forms of linear and angular momentum balance are given by

$$\mathbf{n}'(s) \;=\; \mathbf{0} \tag{2.6}$$

and

$$\mathbf{m}'(s) \;+\; \mathbf{r}'(s)\times\mathbf{n}(s) \;=\; \mathbf{0}, \tag{2.7}$$

for all $s \in [-\frac{1}{2},\frac{1}{2}]$. Next we express the fields $\mathbf{n}$ and $\mathbf{m}$ also in terms of convected components:

$$\mathbf{n} \;=\; n_i\mathbf{d}_i \quad\text{and}\quad \mathbf{m} \;=\; m_i\mathbf{d}_i. \tag{2.8}$$

Let $\mathcal{D} \;:=\; \mathbb{R}^2\times(0,\infty)\times\mathbb{R}^3$. For homogeneous *hyperelastic* rods, we assume the existence of a *stored-energy function* $W:\mathcal{D}\to\mathbb{R}$, *viz.*, $W(\nu_1,\nu_2,\nu_3,\kappa_1,\kappa_2,\kappa_3)$, such that

$$n_j \;=\; \frac{\partial W}{\partial \nu_j} \quad\text{and}\quad m_j \;=\; \frac{\partial W}{\partial \kappa_j}, \quad j \;=\; 1,2,3. \tag{2.9}$$

We henceforth assume that W is sufficiently smooth (of class C^k, $k\geq 3$). If we define the triples $\mathsf{n}=(n_1,n_2,n_3)$, $\mathsf{m}=(m_1,m_2,m_3)$, $\mathsf{v}=(\nu_1,\nu_2,\nu_3)$, and $\mathsf{k}=(\kappa_1,\kappa_2,\kappa_3)$, and also $\mathsf{W}(\mathsf{v},\mathsf{k})=W(\nu_1,\nu_2,\nu_3,\kappa_1,\kappa_2,\kappa_3)$, then (2.9) takes the compact form

$$\mathsf{n} \;=\; \frac{\partial \mathsf{W}}{\partial \mathsf{v}} \quad\text{and}\quad \mathsf{m} \;=\; \frac{\partial \mathsf{W}}{\partial \mathsf{k}}. \tag{2.10}$$

Next we discuss material (cross-sectional) symmetry. Let let $\mathsf{R}_\theta \in \widetilde{SO}(2)$ denote the rotation matrix

$$\mathsf{R}_\theta \;=\; \begin{bmatrix} \cos\theta & -\sin\theta & 0\\ \sin\theta & \cos\theta & 0\\ 0 & 0 & 1\end{bmatrix}. \tag{2.11}$$

We say that the rod is transversely *hemitropic* if

$$\mathsf{W}(\mathsf{R}_\theta\mathsf{v},\mathsf{R}_\theta\mathsf{k}) \;=\; \mathsf{W}(\mathsf{v},\mathsf{k}) \quad \text{for all } \theta\in\mathbb{R} \;(\mathrm{mod}\, 2\pi) \tag{2.12}$$

and *flip symmetric* if

$$\mathsf{W}(\mathsf{E}\mathsf{v},\mathsf{E}\mathsf{k}) \;=\; \mathsf{W}(\mathsf{v},\mathsf{k}), \tag{2.13}$$

where E denotes the reflection matrix

$$\mathsf{E} \;=\; \begin{bmatrix} 1 & 0 & 0\\ 0 & -1 & 0\\ 0 & 0 & 1\end{bmatrix}. \tag{2.14}$$

Flip-symmetric, hemitropic rods can be rigorously derived from corresponding rods having the material symmetry of a regular, cylindrical helix, in the limit that the pitch of the helix goes to zero [8].

By contrast, a rod is said to be transversely *isotropic* if it is transversely hemitropic and, in addition, the stored-energy function satisfies

$$\mathsf{W}(\mathsf{E}\mathsf{v},-\mathsf{E}\mathsf{k}) \;=\; \mathsf{W}(\mathsf{v},\mathsf{k}), \tag{2.15}$$

with E as defined in (2.14). Note the appearance of the minus sign in the second argument above, which arises due to the change in orientation under the reflection E; cf. [7]. No such change of sign occurs in (2.13) since the underlying symmetry of the flip is a proper rotation; cf. [7], [8].

In this work, we consider only flip-symmetric, hemitropic rods that are also *unshearable*, for which the constraints $\nu_\alpha = 0$ are enforced or, equivalently,

$$\mathbf{r}' \;=\; \lambda \mathbf{d}_3 \tag{2.16}$$

is imposed. From (2.12), (2.13), and a representation theorem of Cauchy [2], we find that the stored energy function for an unshearable hemitropic rod has the representation

$$W(\nu_i, \kappa_i) \;=\; \Upsilon(\kappa_\alpha \kappa_\alpha, \kappa_3, \nu_3), \tag{2.17}$$

where we employ the convention that repeated Greek indices imply summation from 1 to 2. We henceforth assume that the 4×4 Hessian matrix,

$$\mathsf{H} \;=\; \begin{bmatrix} \mathsf{W}_{\nu_3\nu_3}(\cdot) & \mathsf{W}_{\nu_3 \mathsf{k}}(\cdot) \\ \mathsf{W}_{\mathsf{k}\nu_3}(\cdot) & \mathsf{W}_{\mathsf{kk}}(\cdot) \end{bmatrix}, \tag{2.18}$$

is positive definite on $(0, \infty) \times \mathbb{R}^3$. Then the vector field $n_\alpha \mathbf{d}_\alpha$ is the Lagrange multiplier that enforces the constraint (2.16).

3. Equilibria of the fixed-free rod. In this section we consider a general class of axially loaded, unshearable, transversely hemitropic, *fixed-free* rods, as depicted in Figure 2. These rods are completely fixed ("welded") to allow no displacement or rotation at the end $s = -\frac{1}{2}$ and are subjected to a horizontal, compressive "dead load", $-P\mathbf{e}_3$, at the end $s = \frac{1}{2}$, which is otherwise unconstrained.

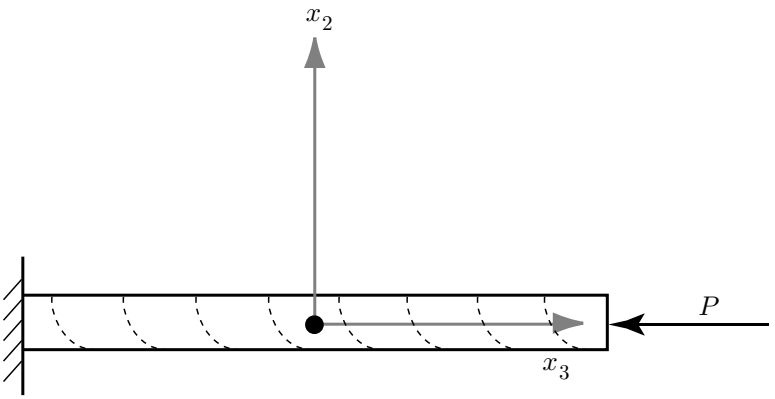

FIG. 2. Schematic of the fixed-free rod

Here we demonstrate that *all equilibria of the nonlinear problem are planar*. By *planar* we mean that the field $\mathbf{r}$ belongs to a two-dimensional subspace of $\mathbb{E}^3$. This is striking, for it demonstrates that hemitropy by itself is insufficient to cause nonplanarity.

By virtue of (2.17) and (2.18) we have

$$\hat{\Upsilon}_{,1}(\kappa_\alpha \kappa_\alpha, \kappa_3, \nu_3) \;>\; 0 \tag{3.1}$$

for all $(\nu_3, \kappa_i) \in (0,\infty) \times \mathbb{R}^3$, where $\hat{\Upsilon}_{,1} = \frac{\partial \hat{\Upsilon}}{\partial(\kappa_\alpha \kappa_\alpha)}$. This boundary value problem is comprised of the field equations (2.6) - (2.10), (2.16) - (2.17), and (3.1), and the boundary conditions

$$\mathbf{r}(-\frac{1}{2}) \;=\; \mathbf{0}, \quad \mathbf{d}_i(-\frac{1}{2}) \;=\; \mathbf{e}_i, \quad i = 1,2,3, \tag{3.2}$$

$$\mathbf{n}(\frac{1}{2}) \;=\; -P\mathbf{e}_3, \quad \mathbf{m}(\frac{1}{2}) \;=\; \mathbf{0}. \tag{3.3}$$

Observe that integration of (2.6) using $(3.3)_1$ yields

$$\mathbf{n} \;\equiv\; -P\mathbf{e}_3, \tag{3.4}$$

and then integration of (2.7) leads to

$$\mathbf{m} \;-\; P\mathbf{r} \times \mathbf{e}_3 \;\equiv\; \mathbf{c}. \tag{3.5}$$

Taking the dot product of (3.5) with $\mathbf{e}_3$ reveals that

$$\mathbf{e}_3 \cdot \mathbf{m} \;\equiv \mathbf{e}_3 \cdot \mathbf{c}, \tag{3.6}$$

which together with $(3.3)_2$ implies that

$$\mathbf{e}_3 \cdot \mathbf{m} \;\equiv\; 0. \tag{3.7}$$

Next we introduce a semi-convected basis field (similar to that employed in the usual analysis of the Lagrange top; cf. [16]) as follows:

$$\begin{aligned} \mathbf{a}_1 &= \cos\theta(\cos\psi\mathbf{e}_1 \;+\; \sin\psi\mathbf{e}_2) \;-\; \sin\theta\mathbf{e}_3, \\ \mathbf{a}_2 &= -\sin\psi\mathbf{e}_1 \;+\; \cos\psi\mathbf{e}_2, \\ \mathbf{d}_3 \;=\; \mathbf{a}_3 &= \sin\theta(\cos\psi\mathbf{e}_1 \;+\; \sin\psi\mathbf{e}_2) \;+\; \cos\theta\mathbf{e}_3, \end{aligned} \tag{3.8}$$

where ψ is the right-handed polar angle between $\mathbf{e}_1$ and the unit vector $\hat{\mathbf{e}}_1 = \cos\psi\mathbf{e}_1 + \sin\psi\mathbf{e}_2$, and θ denotes the angle between $\mathbf{e}_3$ and $\mathbf{d}_3 = \mathbf{a}_3$. The rationale for these definitions lies in the fact that $\mathbf{d}_3 \in \text{span}\{\hat{\mathbf{e}}_1, \mathbf{e}_3\}$, and if $\psi'(s) \equiv 0$, then $\mathbf{d}_3$ lies within a fixed plane. Since $\mathbf{r}' = \lambda\mathbf{d}_3$, by (2.16), it follows that $\mathbf{r}'$, and hence $\mathbf{r}$, lies in a fixed plane, and hence the solution is planar. The following calculations demonstrate that indeed either $\mathbf{d}_3 \equiv \mathbf{e}_3$ or $\psi' \equiv 0$, from which planarity follows.

Differentiation of relations (3.8) yields

$$\mathbf{a}_i' \;=\; \boldsymbol{\omega} \times \mathbf{a}_i, \quad i \;=\; 1,2,3, \tag{3.9}$$

where

$$\boldsymbol{\omega} \;=\; -\psi' \sin\theta\mathbf{a}_1 \;+\; \theta'\mathbf{a}_2 \;+\; \psi'\cos\theta\mathbf{a}_3. \tag{3.10}$$

We also introduce another (Euler) angle ϕ that relates the $\mathbf{a}_i$ to the directors $\mathbf{d}_i$, as follows:

$$\begin{aligned} \mathbf{a}_1 &= \cos\phi\mathbf{d}_1 \;-\; \sin\phi\mathbf{d}_2, \\ \mathbf{a}_2 &= \sin\phi\mathbf{d}_1 \;+\; \cos\phi\mathbf{d}_2, \end{aligned} \tag{3.11}$$

and we then have

$$\begin{aligned} \boldsymbol{\kappa} &= \boldsymbol{\omega} \;+\; \phi'\mathbf{d}_3 \\ &= \psi'\sin\theta\mathbf{a}_1 \;+\; \theta'\mathbf{a}_2 \;+\; (\psi'\cos\theta + \phi')\mathbf{d}_3, \end{aligned} \tag{3.12}$$

where, again, $\boldsymbol{\kappa}$ is such that $\mathbf{d}_i' = \boldsymbol{\kappa} \times \mathbf{d}_i$, as defined in (2.3). We note, in passing, that (3.12) is consistent with equations (8) on p. 386 of [11].

Inverting (3.8) to obtain

$$\mathbf{e}_3 \;=\; -\sin\theta\mathbf{a}_1 \;+\; \cos\theta\mathbf{a}_3, \tag{3.13}$$

recalling (3.4), and employing $\{\mathbf{a}_1, \mathbf{a}_2, \mathbf{a}_3 = \mathbf{d}_3\}$ as a fundamental basis, we obtain the following expressions:

$$\begin{aligned} \mathbf{n} &= P(\sin\theta\mathbf{a}_1 \;-\; \cos\theta\mathbf{a}_3), \\ \mathbf{m} &= \overline{m}_\alpha\mathbf{a}_\alpha \;+\; m_3\mathbf{d}_3, \\ \boldsymbol{\kappa} &= \overline{\kappa}_\alpha\mathbf{a}_\alpha \;+\; \kappa_3\mathbf{d}_3, \\ \boldsymbol{\omega} &= \overline{\kappa}_\alpha\mathbf{a}_\alpha \;+\; \omega_3\mathbf{d}_3. \end{aligned} \tag{3.14}$$

Substitution of (2.16) and (3.14) into the moment balance equation (2.7) yields

$$\begin{aligned} \overline{m}_1' \;-\; \overline{m}_2\omega_3 \;+\; m_3\overline{\kappa}_2 &= 0, \\ \overline{m}_2' \;+\; \overline{m}_1\omega_3 \;-\; m_3\overline{\kappa}_1 \;+\; \lambda P\sin\theta &= 0, \\ m_3' \;-\; \overline{m}_1\overline{\kappa}_2 \;+\; \overline{m}_2\overline{\kappa}_1 &= 0, \end{aligned} \tag{3.15}$$

where the components ω_3 and $\overline{\kappa}_\alpha$ are as defined in (3.10) and (3.12), respectively. Noting the invariance $\overline{\kappa}_\alpha\overline{\kappa}_\alpha = \kappa_\alpha\kappa_\alpha$, we deduce from (2.9) and (2.17) that

$$\overline{m}_\beta \;=\; 2\hat{\Upsilon}_{,1}(\overline{\kappa}_\alpha\overline{\kappa}_\alpha, \kappa_3, \lambda)\overline{\kappa}_\beta, \quad \beta \;=\; 1, 2. \tag{3.16}$$

Substitution of (3.16) into $(3.15)_3$ reveals that $m_3'(s) \equiv 0$, and finally, upon imposing the boundary condition $(3.3)_2$, we find that

$$m_3 \equiv 0. \tag{3.17}$$

Then, recalling (3.7) and employing (3.13) with $\mathbf{a}_3 = \mathbf{d}_3$, we compute

$$\begin{aligned} 0 &= \mathbf{m}\cdot\mathbf{e}_3 \\ &= (\overline{m}_1\mathbf{a}_1 \;+\; \overline{m}_2\mathbf{a}_2)\cdot(-\sin\theta\mathbf{a}_1 \;+\; \cos\theta\mathbf{d}_3) \\ &= -\overline{m}_1\sin\theta. \end{aligned} \tag{3.18}$$

Thus, either $\sin\theta \equiv 0$ or $\overline{m}_1 \equiv 0$.

In the first case, suppose $\sin\theta \equiv 0$. Then (3.8) implies that $\mathbf{d}_3 = \mathbf{e}_3$. Since $\mathbf{r}' = \lambda\mathbf{d}_3$ by (2.16), it follows that $\mathbf{r}' = \lambda\mathbf{e}_3$, i.e. the rod is *straight* (parallel to the constant vector $\mathbf{e}_3$) and thus planar.

In the second case, observe from (3.1) and (3.16) that $\bar{m}_1 = 0 \Leftrightarrow \bar{\kappa}_1 = 0$. Thus from (3.12) we find that

$$\psi'\sin\theta = 0, \tag{3.19}$$

from which we immediately conclude that $\psi' \equiv 0$. This implies that ψ is constant, and as was indicated near the beginning of this section, this also implies that the rod must be planar. Thus we have proved the following:

THEOREM 3.1. All equilibria of an axially loaded, unshearable, hemitropic, "fixed-free" rod are planar.

REMARK 3.2. The proof of Theorem 3.1 depends crucially on (2.16), which is the assumption of unshearability, or $\mathbf{r}' = \lambda \mathbf{d}_3$. Equilibria of shearable rods may, perhaps, be nonplanar.

We conclude this section by summarizing the remaining field equations governing the planar equilibria. We exclude the trivial case $\sin\theta \equiv 0$, which we demonstrated would imply that the rod remain straight. Due to the rotational symmetry in our problem, without loss of generality, we may choose $\psi \equiv 0$, in which case (3.8), (3.10), and (3.12) specialize to

$$\begin{aligned} \mathbf{a}_1 &= \cos\theta \mathbf{e}_1 - \sin\theta \mathbf{e}_3, \\ \mathbf{a}_2 &= \mathbf{e}_2, \\ \mathbf{d}_3 = \mathbf{a}_3 &= \sin\theta \mathbf{e}_1 + \cos\theta \mathbf{e}_3, \end{aligned} \tag{3.20}$$

and

$$\omega = \theta' \mathbf{a}_2 \quad \text{and} \quad \boldsymbol{\kappa} = \theta' \mathbf{a}_2 + \phi' \mathbf{d}_3, \tag{3.21}$$

respectively. With this choice, by virtue of (3.17) and the fact that $\overline{m}_1 = 0$, both $(3.15)_1$ and $(3.15)_3$ vanish identically, while $(3.15)_2$ becomes

$$2[\hat{\Upsilon}_{,1}((\theta')^2, \phi', \lambda)\theta']' + \lambda P \sin\theta = 0. \tag{3.22}$$

Now (3.4) and $(3.20)_3$ imply that

$$n_3 = \mathbf{n} \cdot \mathbf{d}_3 = -P \mathbf{e}_3 \cdot \mathbf{d}_3 = -P \cos\theta. \tag{3.23}$$

Using (2.9), (2.17), and (3.17) we obtain

$$n_3 = \hat{\Upsilon}_{,3}((\theta')^2, \phi', \lambda) = -P \cos\theta \tag{3.24}$$

and

$$m_3 = \hat{\Upsilon}_{,2}((\theta')^2, \phi', \lambda) = 0. \tag{3.25}$$

From $(3.2)_2$ and $(3.20)_3$, it follows that

$$\cos\theta(-\frac{1}{2}) = 0, \tag{3.26}$$

and from $(3.3)_2$ and (3.16), we have

$$\begin{aligned} \mathbf{m}(\frac{1}{2}) \cdot \mathbf{d}_2 &= m_2(\frac{1}{2}) = 0 \\ &\Leftrightarrow \ \overline{\kappa}_2 = 0 \\ &\Leftrightarrow \ \theta'(\frac{1}{2}) = 0. \end{aligned} \tag{3.27}$$

Field equations (3.22), (3.24), and (3.25), together with boundary conditions (3.26) and (3.27), determine the planar equilibria of the rod. In view of (2.17) and (2.18), we conclude that (3.24) and (3.25) determine λ and ϕ' uniquely in terms of P, θ and θ', substitution of which into (3.22) yields a standard "generalized" elastica problem, amenable to detailed analysis. We do not pursue this here, but refer to [1] (and the references therein) for the analysis of similar problems for planar, nonlinearly elastic rods.

4. The fixed-fixed rod: Governing equations, symmetry, and linearized solutions. The *fixed-fixed* rod that we consider is clamped at each end and guided by rollers that prevent displacement perpendicular to the $\mathbf{e}_3$ axis and all rotation. End displacements of equal magnitude and opposite direction along the $\mathbf{e}_3$-axis are specified by the parameter $\lambda \in (0, \infty)$, which represents the distance between the two ends; cf. Figure 3.

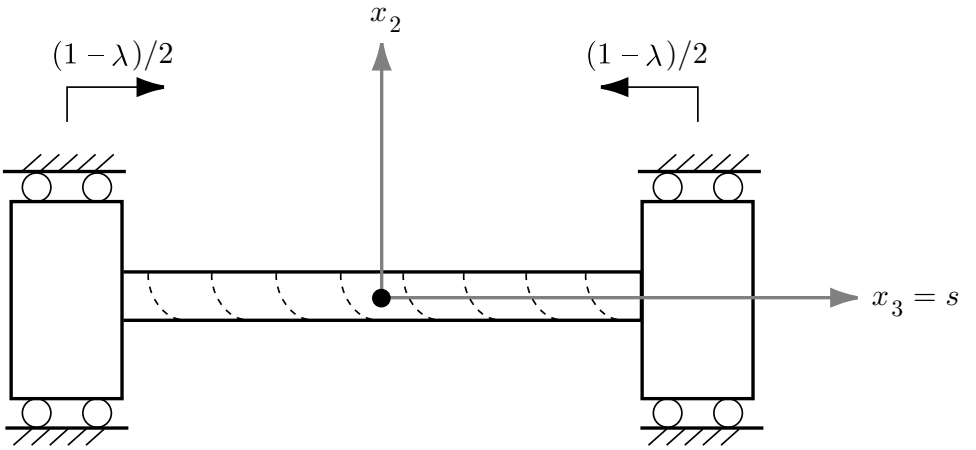

FIG. 3. Schematic of the fundamental problem

4.1. *Governing equations.* We again consider hemitropic, unshearable rods. For definiteness, we choose a specific class of hemitropy that allows both chirality and infinite compressive force under ultimate compression, governed by the following stored energy function:

$$\Upsilon \;=\; \frac{1}{2}[C\kappa_\alpha\kappa_\alpha + B\kappa_3^2 + \Phi(\nu_3) + 2A\kappa_3(\nu_3 - 1)]. \tag{4.1}$$

From (2.9) the following consitutive equations direcly follow:

$$\begin{aligned} n_3 &= g(\nu_3) \;+\; A\kappa_3, \\ m_3 &= A(\nu_3 - 1) \;+\; B\kappa_3, \\ m_\alpha &= C\kappa_\alpha, \end{aligned} \tag{4.2}$$

where $g := \Phi' : (0, \infty) \to \mathbb{R}$. In view of (2.18), and accounting for unshearability, we see that the moduli $B, C > 0$, and $g'(\cdot) > 0$ on $(0, \infty)$. Assumption (2.18) also implies that $g'(\nu)B - A^2 > 0$ for all $\nu \in (0, \infty)$. We further assume that $g(\nu) \to -\infty$ as $\nu \to 0$.

The modulus A represents the degree of hemitropy inherent in the rod and has no restriction on its sign. As discussed in [7], the sign of A governs the *chirality* or "handedness" of the rod. Note that the rod is isotropic if $A = 0$. The moduli B and C represent the twisting and bending stiffness, respectively, and are each positive. Near the trivial solution and when $A = 0$, B and C respectively correspond exactly to modulus of rigidity "GJ" and bending stiffness "EI", as typically denoted in linear beam theory [15]. Note that equations $(4.2)_{1,2}$ explicitly reveal a coupling of extension and twist.

Upon substituting the constitutive laws (4.2) into the general field equations (2.6) and (2.7), and nondimensionalizing the equations such that $C = 1$, the boundary value

problem for the fixed-fixed rod becomes

$$\frac{d}{ds}\Big[n_\alpha(s)\mathbf{Re}_\alpha(s) \;+\; \Big(g(\nu_3(s)) + A\kappa_3(s)\Big)\mathbf{Re}_3(s)\Big] \;=\; \mathbf{0}, \tag{4.3}$$

$$\begin{aligned}\frac{d}{ds}\Big[\kappa_\alpha(s)\mathbf{Re}_\alpha(s) \;+\; \Big(A(\nu_3(s)-1) + B\kappa_3(s)\Big)\mathbf{Re}_3(s)\Big]& \\ +\; \mathbf{r}'(s)\times\Big[n_\alpha(s)\mathbf{Re}_\alpha(s) \;+\; \Big(g(\nu_3(s)) + A\kappa_3(s)\Big)\mathbf{Re}_3(s)\Big] \;&=\; \mathbf{0},\end{aligned} \tag{4.4}$$

$$\mathbf{r}'(s)\cdot\mathbf{Re}_\alpha(s) \;=\; 0, \tag{4.5}$$

$$\mathbf{r}(\pm\frac{1}{2}) \;=\; \frac{\pm\lambda}{2}\mathbf{e}_3, \tag{4.6}$$

$$\mathbf{R}(\pm\frac{1}{2}) \;=\; \mathbf{I} \tag{4.7}$$

for $s \in (-\frac{1}{2}, \frac{1}{2})$. Note that here we enforce the unshearability explicitly via (4.5) and that the last term in (4.4) vanishes due to the fact that $\mathbf{Re}_3$ is parallel to $\mathbf{r}'$.

With the aid of (2.1) and (2.4), equations (4.3) - (4.7) define a mapping of differentiable functions $\mathbf{x} = (\mathbf{r}, \mathbf{R}, n_\alpha)$, $\alpha = 1, 2$, in

$$\mathcal{X} \equiv \{C^1([-\frac{1}{2}, \frac{1}{2}], \mathbb{E}^3 \times SO(3) \times \mathbb{R}^2) \text{ s.t. (4.6) and (4.7) hold}\}$$

into $\mathcal{Y} \equiv C^0([-\frac{1}{2}, \frac{1}{2}], \mathbb{E}^3 \times \mathbb{E}^3 \times \mathbb{R}^2)$. Denoting this mapping via $\mathcal{F} : \mathbb{R} \times \mathcal{X} \to \mathcal{Y}$, we may represent (4.3) - (4.7) abstractly via

$$\mathcal{F}(\lambda, \mathbf{x}) \;=\; 0. \tag{4.8}$$

4.2. *Symmetries and equivariance properties.* The fixed-fixed rod possesses important symmetry properties that are exploited in our analysis. It is straightforward to show (cf. [14]) that the mapping (4.8) is *equivariant* with respect to the group consisting of arbitrary rotations of magnitude θ about the $\mathbf{e}_3$ axis and rotations by π about any axis perpendicular to $\mathbf{e}_3$ at the center of the rod. By equivariance we mean here that the nonlinear mapping $\mathcal{F}(\lambda, \cdot)$ commutes with the group action as follows:

$$\mathcal{F}(\lambda, \Gamma\mathbf{x}) \;=\; \tilde{\Gamma}\mathcal{F}(\lambda, \mathbf{x}), \tag{4.9}$$

for all $\Gamma \in \{\mathcal{Q}_\theta, \mathcal{E}\mathcal{Q}_\theta : \mathcal{X} \to \mathcal{X},\ 0 \le \theta < 2\pi\}$ and for all $\tilde{\Gamma} \in \{\tilde{\mathcal{Q}}_\theta, \tilde{\mathcal{E}}\tilde{\mathcal{Q}}_\theta : \mathcal{Y} \to \mathcal{Y},\ 0 \le \theta < 2\pi\}$. Table 1 provides explicit representations of these symmetry operations on the field variables $(\mathbf{r}, \mathbf{R}, n_\alpha)$ and other relevant quantities.

TABLE 1. Symmetry transformations.

Quantity $\mathbf{q}$	$\mathcal{Q}_\theta\mathbf{q}$	$\mathcal{E}\mathbf{q}$
$\mathbf{r}(s)$	$\mathbf{Q}_\theta\mathbf{r}(s)$	$\mathbf{E}\mathbf{r}(-s)$
$\mathbf{R}(s)$	$\mathbf{Q}_\theta\mathbf{R}(s)\mathbf{Q}_\theta^T$	$\mathbf{E}\mathbf{R}(-s)\mathbf{E}$
$n_\alpha(s)$	$(Q_\theta)_{\alpha\beta}n_\beta(s)$	$-E_{\alpha\beta}n_\beta(-s)$
$\nu_3(s)$	$(Q_\theta)_{3j}\nu_j(s)$	$-E_{3j}\nu_j(-s)$
$\kappa_i(s)$	$(Q_\theta)_{ij}\kappa_j(s)$	$-E_{ij}\kappa_j(-s)$

In Table 1 the tensors $\mathbf{Q}_\theta$ and $\mathbf{E}$ are defined by their components relative to the fixed basis via

$$[\mathbf{Q}_\theta] \;=\; \begin{bmatrix} \cos\theta & \sin\theta & 0 \\ -\sin\theta & \cos\theta & 0 \\ 0 & 0 & 1 \end{bmatrix}, \qquad [\mathbf{E}] \;=\; \begin{bmatrix} 1 & 0 & 0 \\ 0 & -1 & 0 \\ 0 & 0 & -1 \end{bmatrix}. \tag{4.10}$$

Note that the boundary conditions (4.6) and (4.7) are invariant under all group actions $\Gamma(\mathbf{r}, \mathbf{R}, n_\alpha)$. The action $\tilde{\Gamma}$ on (4.3) - (4.5) is defined as follows: for the first two arguments, corresponding to the two vector-valued equations (4.3) - (4.4), the action is the same as that indicated for $\mathbf{r}$ in Table 1; the two scalar equations in (4.5) transform like $\kappa_\alpha, \alpha = 1, 2$, respectively, in Table 1.

The transformations $\mathcal{Q}_\theta$ (and $\tilde{\mathcal{Q}}_\theta$) and $\mathcal{E}$ (and $\tilde{\mathcal{E}}$) represent proper rotations. In particular, the symmetry operation $\mathcal{E}$ is isomorphic to $\mathbb{Z}_2$ and represents a "flip" (rotation of π radians) about the x axis. Therefore, the underlying equations are equivariant with respect to representations of $SO(2) \oplus \mathbb{Z}_2 = O(2) \subset SO(3)$. The actions of $O(2)$ appearing in (4.9) are each faithful on $\mathcal{X}$ and $\mathcal{Y}$, respectively. As will be seen, the presence of the flip $\mathcal{E}$ is essential for our analysis.

4.3. *Linearized equations.* Observe that for any $\lambda \in (0, \infty)$ the following *straight* solution satisifies the boundary value problem (BVP) (4.3) - (4.7):

$$\mathbf{r}(s) \;\equiv\; \lambda s \mathbf{e}_3, \qquad \mathbf{R}(s) \;\equiv\; \mathbf{I}, \qquad n_\alpha(s) \;\equiv\; 0. \tag{4.11}$$

It follows that $\mathbf{r}' \equiv \lambda \mathbf{e}_3$, $\nu_\alpha \equiv 0$, $\nu_3 \equiv \lambda$, and $\kappa_i \equiv 0, i = 1, 2, 3$. Physically, under such straight solutions, the rod undergoes change of length but does not twist, bend, or shear. Note further that within the family of straight solutions, the rod develops both a uniform internal axial force $\mathbf{n}(s) = g(\lambda)\mathbf{e}_3$ and an internal axial twisting torque $\mathbf{m}(s) = A(\lambda - 1)\mathbf{e}_3$.

The linearization of the BVP (4.3) - (4.7) is obtained by perturbing the straight solution as follows:

$$\mathbf{r}(s) \;=\; \lambda s \mathbf{e}_3 + \epsilon \boldsymbol{\rho}(s), \qquad \mathbf{R}(s) \;= exp[\epsilon \boldsymbol{\Psi}(s)], \qquad n_\alpha(s) \;=\; \epsilon \eta_\alpha(s), \tag{4.12}$$

where $\boldsymbol{\Psi}$ is a skew-symmetric tensor field with axial vector $\boldsymbol{\psi} \equiv axial(\boldsymbol{\Psi})$, i.e., $\boldsymbol{\psi}(s) \times \mathbf{v} \equiv \boldsymbol{\Psi}(s)\mathbf{v}$ for all $\mathbf{v} \in \mathbb{E}$. Substituting (4.12) into (4.3) - (4.7) and retaining only terms of first order in ϵ yields the linearize BVP:

$$\begin{aligned}
\eta'_\alpha \mathbf{e}_\alpha \;+\; g(\lambda)\boldsymbol{\psi}' \times \mathbf{e}_3 \;&=\; \mathbf{0}, && (4.13)\\
(g'(\lambda)\boldsymbol{\rho}'' \;+\; A\boldsymbol{\psi}'') \cdot \mathbf{e}_3 \;&=\; 0, && (4.14)\\
\boldsymbol{\psi}'' \cdot \mathbf{e}_\alpha \mathbf{e}_\alpha \;+\; A(\lambda - 1)\boldsymbol{\psi}' \times \mathbf{e}_3 & \\
+\; g(\lambda)\boldsymbol{\rho}' \times \mathbf{e}_3 \;+\; \lambda \mathbf{e}_3 \times (\eta_\alpha \mathbf{e}_\alpha + g(\lambda)\boldsymbol{\psi} \times \mathbf{e}_3) \;&=\; \mathbf{0}, && (4.15)\\
(A\boldsymbol{\rho}'' + B\boldsymbol{\psi}'') \cdot \mathbf{e}_3 \;&=\; 0, && (4.16)\\
(\boldsymbol{\rho}' - \lambda \boldsymbol{\psi} \times \mathbf{e}_3) \cdot \mathbf{e}_\alpha \;&=\; 0, && (4.17)\\
\boldsymbol{\rho}(\pm\frac{1}{2}) \;&=\; \mathbf{0}, && (4.18)\\
\boldsymbol{\psi}(\pm\frac{1}{2}) \;&=\; \mathbf{0}. && (4.19)
\end{aligned}$$

Equations (4.14) and (4.16), boundary conditions (4.18) and (4.19), and the convexity condition (2.18) (cf. (2.17) and (4.1)) imply that $\boldsymbol{\rho}$ and $\boldsymbol{\psi}$ lie in $span\{\mathbf{e}_1, \mathbf{e}_2\}$.

Next we substitute (4.17) and the integral of (4.13) into (4.15), yielding

$$\boldsymbol{\psi}'' \ + \ A(\lambda-1)\boldsymbol{\psi}' \times \mathbf{e}_3 \ - \ \lambda g(\lambda)\boldsymbol{\psi} \ \ = \ \ \lambda \mathbf{c} \times \mathbf{e}_3, \tag{4.20}$$

where $\mathbf{c} \in span\{\mathbf{e}_1, \mathbf{e}_2\}$ is the constant of integration coming from (4.13). Observe that the integral of (4.17), with the aid of (4.18), implies

$$\int_{-\frac{1}{2}}^{\frac{1}{2}} \boldsymbol{\psi}(s) \ ds \ = \mathbf{0}. \tag{4.21}$$

Then the integral of (4.20), together with (4.19) and (4.21), gives

$$\boldsymbol{\psi}'(\frac{1}{2}) - \boldsymbol{\psi}'(-\frac{1}{2}) \ = \ \lambda \mathbf{c} \times \mathbf{e}_3, \tag{4.22}$$

i.e., (4.20), (4.22) and (4.19) lead to the following stand-alone BVP for $\boldsymbol{\psi}$:

$$\boldsymbol{\psi}'' \ + \ A(\lambda-1)\boldsymbol{\psi}' \times \mathbf{e}_3 \ - \ \lambda g(\lambda)\boldsymbol{\psi} \ \ = \ \ \boldsymbol{\psi}'(\frac{1}{2}) - \boldsymbol{\psi}'(-\frac{1}{2}), \tag{4.23}$$

$$\boldsymbol{\psi}(\pm\frac{1}{2}) \ \ = \ \ \mathbf{0}. \tag{4.24}$$

Once we solve (4.23) and (4.24), the other perturbative fields in (4.12) are determined by back-substitution into (4.17) and (4.13):

$$\boldsymbol{\rho}(s) \ = \ \lambda \int_{-\frac{1}{2}}^{s} \psi(\tau) \ d\tau \times \mathbf{e}_3 \tag{4.25}$$

and

$$\eta_\alpha(s)\mathbf{e}_\alpha \ = \ g(\lambda)\mathbf{e}_3 \times \boldsymbol{\psi}(s) \ + \ \mathbf{e}_3 \times \frac{\boldsymbol{\psi}'(\frac{1}{2}) - \boldsymbol{\psi}'(-\frac{1}{2})}{\lambda}. \tag{4.26}$$

Defining coefficients

$$a \ = \ \tilde{a}(\lambda) \ = \ A(\lambda-1), \qquad \Omega \ = \tilde{\Omega}(\lambda) \ = \ -\lambda g(\lambda), \tag{4.27}$$

we rewrite (4.23) as

$$\boldsymbol{\psi}''(s) \ + \ a\boldsymbol{\psi}'(s) \times \mathbf{e}_3 \ + \ \Omega\boldsymbol{\psi}(s) \ = \ \boldsymbol{\psi}'(\frac{1}{2}) - \boldsymbol{\psi}'(-\frac{1}{2}). \tag{4.28}$$

We now define the "spatial frequencies" ω_1 and ω_2 as

$$\omega_1 \ = \ \frac{a + \sqrt{a^2 + 4\Omega}}{2}, \qquad \omega_2 \ = \ \frac{a - \sqrt{a^2 + 4\Omega}}{2}, \tag{4.29}$$

and we note that

$$a \ = \ \omega_1 + \omega_2, \qquad \Omega \ = \ -\omega_1\omega_2. \tag{4.30}$$

For $a^2 + 4\Omega \geq 0$, the general solution of (4.28) is, in component form w.r.t. $\{\mathbf{e}_1, \mathbf{e}_2\}$,

$$\begin{aligned}[\boldsymbol{\psi}(s)] \ \ = \ \ & C_1 \begin{bmatrix} \cos(\omega_1 s) - \frac{2\omega_1}{\Omega} \sin\frac{\omega_1}{2} \\ \sin(\omega_1 s) \end{bmatrix} \ + \ C_2 \begin{bmatrix} \cos(\omega_2 s) - \frac{2\omega_2}{\Omega} \sin\frac{\omega_2}{2} \\ \sin(\omega_2 s) \end{bmatrix} \\ & C_3 \begin{bmatrix} \sin(\omega_1 s) \\ -\cos(\omega_1 s) + \frac{2\omega_1}{\Omega} \sin\frac{\omega_1}{2} \end{bmatrix} \ + \ C_4 \begin{bmatrix} \sin(\omega_2 s) \\ -\cos(\omega_2 s) + \frac{2\omega_2}{\Omega} \sin\frac{\omega_2}{2} \end{bmatrix}. \end{aligned} \tag{4.31}$$

REMARK 4.1. It is also possible to write the general solution of (4.28) for the case $a^2 + 4\Omega < 0$. However, a lengthy but straightforward calculation shows that the solution set of the BVP (4.28) and (4.24) contains only the trivial solution.

The solution set of the BVP (4.28) and (4.24) is a subspace of the span of the general solution (4.31). Due to the presence of the underlying $SO(2)$ symmetry, the dimension of this subspace of solutions must be at least 2, which would generally pose problems in bifurcation analysis. These problems are overcome, however, by exploiting equivariance.

In view of (4.9), we may rigorously restrict $\mathcal{F}(\lambda, \cdot)$ in (4.8) to a fixed-point space corresponding to any subgroup of $O(2)$, e.g., [6]. We choose to work in the fixed-point space of functions that are invariant under the "flip" $\mathcal{E}$, i.e. $\{\mathbf{x} = (\mathbf{r}, \mathbf{R}, n_\alpha, \alpha = 1, 2) : \mathcal{E}\mathbf{x} = \mathbf{x}\}$. Of course, this restriction is inherited by the linearization, which we now exploit.

4.4. *Linearized solutions using symmetry reduction.* Flip-invariant solutions of the linearized problem (4.13) - (4.19) have the property that $\mathcal{E}(\boldsymbol{\psi}, \boldsymbol{\rho}, \eta_\alpha) = (\boldsymbol{\psi}, \boldsymbol{\rho}, \eta_\alpha)$ for some appropriate action $\mathcal{E}$ of $\mathbb{Z}^2$ representing the flip about $\mathbf{e}_1$. From (4.10) and Table 1 we can read the $\mathbb{Z}^2$ action directly as follows:

$$\mathcal{E}(\boldsymbol{\psi}(s), \boldsymbol{\rho}(s), \eta_\alpha(s)) \;=\; (\mathbf{E}\boldsymbol{\psi}(-s), \mathbf{E}\boldsymbol{\rho}(-s), -E_{\alpha\beta}\eta_\beta(-s)). \tag{4.32}$$

With respect to components relative to the fixed basis, flip-invariance is then equivalent to

$$\begin{aligned} \rho_1(s) &= \rho_1(-s), & \rho_2(s) &= -\rho_2(-s), \\ \psi_1(s) &= \psi_1(-s), & \psi_2(s) &= -\psi_2(-s), \\ \eta_1(s) &= -\eta_1(-s), & \eta_2(s) &= \eta_2(-s). \end{aligned} \tag{4.33}$$

Returning to the general solution (4.31) of (4.28), we see that $(4.33)_2$ holds iff $C_3 = C_4 = 0$, i.e., the general solutions of the reduced problem in the fixed-point space is given by

$$[\boldsymbol{\psi}(s)] \;=\; C_1 \begin{bmatrix} \cos(\omega_1 s) - \frac{2\omega_1}{\Omega}\sin\frac{\omega_1}{2} \\ \sin(\omega_1 s) \end{bmatrix} + C_2 \begin{bmatrix} \cos(\omega_2 s) - \frac{2\omega_2}{\Omega}\sin\frac{\omega_2}{2} \\ \sin(\omega_2 s) \end{bmatrix}. \tag{4.34}$$

With this reduction, it is enough to enforce, say, the boundary condition (4.24) at $s = \frac{1}{2}$, $\boldsymbol{\psi}(\frac{1}{2}) = \mathbf{0}$ (the remaining boundary condition $\boldsymbol{\psi}(-\frac{1}{2}) = \mathbf{0}$ follows from $\mathbb{Z}^2$ invariance), yielding the following linear equations in C_1 and C_2:

$$\begin{bmatrix} \cos\frac{\omega_1}{2} - \frac{2\omega_1}{\Omega}\sin\frac{\omega_1}{2} & \cos\frac{\omega_2}{2} - \frac{2\omega_2}{\Omega}\sin\frac{\omega_2}{2} \\ \sin\frac{\omega_1}{2} & \sin\frac{\omega_2}{2} \end{bmatrix} \begin{bmatrix} C_1 \\ C_2 \end{bmatrix} \;=\; \begin{bmatrix} 0 \\ 0 \end{bmatrix}. \tag{4.35}$$

Therefore, nontrivial solutions of the linearized BVP (4.28) and (4.24) that are flip-invariant are in 1-1 correspondence with nontrivial solutions of (4.35).

Before proceeding, we note here a simple yet crucial result that will be used in the ensuing bifurcation analysis.

THEOREM 4.2. The dimension of the space of flip-invariant nontrivial solutions of the BVP (4.28) and (4.24) is at most 1.

Proof. The dimension of the solution space of the linear equations (4.35) is clearly at most 2. If it were 2, then each term of the matrix would be 0. This would necessitate $\sin\frac{\omega_i}{2} = \cos\frac{\omega_i}{2} = 0$ for $i = 1, 2$, which obviously cannot occur. □

Nontrivial solutions of (4.35) occur for values of (a, Ω) for which

$$\begin{vmatrix} \cos\frac{\omega_1}{2} - \frac{2\omega_1}{\Omega}\sin\frac{\omega_1}{2} & \cos\frac{\omega_2}{2} - \frac{2\omega_2}{\Omega}\sin\frac{\omega_2}{2} \\ \sin\frac{\omega_1}{2} & \sin\frac{\omega_2}{2} \end{vmatrix} \;=\; 0. \tag{4.36}$$

Expanding the determinant, the resulting characteristic equation is

$$f(a,\Omega) \;=\; -\omega_1\omega_2 \sin\frac{\omega_1-\omega_2}{2} \;+\; 2(\omega_1-\omega_2)\sin\frac{\omega_1}{2}\sin\frac{\omega_2}{2} \;=\; 0. \tag{4.37}$$

Substituting from (4.29) reveals that solutions of (4.37) lie on a family of *characteristic curves* in the $a-\Omega$ plane, labelled $\mathcal{C}_i$ in Figure 4. These curves intersect the a-axis at the points labelled c_i. Because $f(a,\Omega)$ vanishes identically for $\Omega = 0$, the c_i are determined by expanding $f(a,\Omega)$ about Ω and determining the condition on a for which the leading term (in this case, the second order term) vanishes. As a result, the numbers c_i are determined to be the positive solutions of the equation

$$\tan\frac{a}{2} \;=\; \frac{a}{2}. \tag{4.38}$$

The c_i form a monotone increasing sequence such that $c_1 < c_2 < \ldots$, and they have the property that $c_i \sim (2i+1)\pi$ as $i \to \infty$.

Next, the infinite sequence of intersection points along the Ω-axis coincide with the classical (normalized) buckling loads of a compressed, planar, clamped-clamped rod; cf. [15]. To see this, we set $a = 0$ in (4.37), which in view of (4.29) reduces to

$$\Omega\sin\sqrt{\Omega} - 4\sqrt{\Omega}\sin^2\frac{\sqrt{\Omega}}{2} \;=\; 0$$

or

$$\sin\frac{\sqrt{\Omega}}{2}\Big[\sqrt{\Omega}\cos\frac{\sqrt{\Omega}}{2} - 2\sin\frac{\sqrt{\Omega}}{2}\Big] \;=\; 0. \tag{4.39}$$

Hence, either $\Omega_{2n-1} = (2n\pi)^2$ or $\Omega_{2n} = c_n^2$, $n = 1, 2, 3, \ldots$.

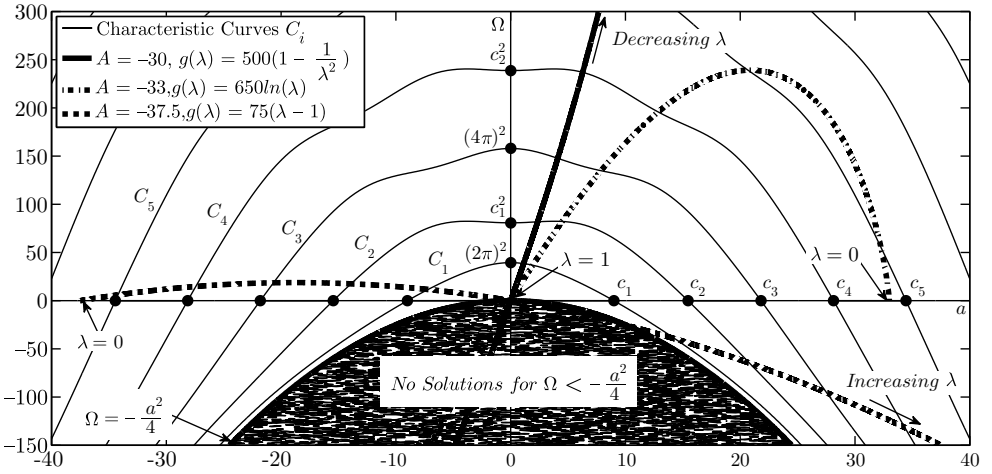

FIG. 4. Characteristic curves and parametric constitutive curves

We summarize below three important properties of the characteristic curves which are suggested by inspection of Figure 4 and which have been verified.

(1) **Nesting of characteristic curves.** The characteristic curves are *nested* - that is, they comprise a family of nonintersecting curves that that montonically emanate away from the origin. The curves can be enumerated $\mathcal{C}_1, \mathcal{C}_2, ...$ such that the region between $\mathcal{C}_1$ and the a-axis contains no other characteristic curves, and the region between $\mathcal{C}_i$ and the a-axis strictly contains $\mathcal{C}_{i-1}$ for $i = 2, 3, 4, ...$

(2) **Exhaustiveness of characteristic curves.** The characteristic curves $\mathcal{C}_i$, $i = 1, 2, ...,$ capture *all* solutions of (4.37). As shown above, the sequence of points $(0, (2\pi)^2)$, $(0, c_1^2)$, $(0, (4\pi)^2)$, $(0, c_2^2)$, ... are the *only* nontrivial points along the Ω-axis that satisfy the characteristic equation, and the curves $\mathcal{C}_i$ are in direct correspondence with these points.

(3) **Symmetry properties.** Figure 4 reveals that each modal curve is symmetrical about the Ω-axis and is equivalent to an invariance of solutions of (4.37) under the transformation $a \to -a$. This transformation is equivalent to a reversal of the hemitropic sense of the rod's material ($A \to -A$) and demonstrates what is intuitively obvious, viz., the emergence of a nontrivial solution should not depend on the sense of the rod's chiralty.

For given constitutive data (4.27), nontrivial flip-invariant solutions of the BVP (4.28) and (4.24) occur whenever $\lambda = \lambda_o$ is a root of the characteristic equation (4.37), viz.,

$$\tilde{f}(\lambda_o) \;\equiv\; f(\tilde{a}(\lambda_o), \tilde{\Omega}(\lambda_o)) \;=\; 0. \tag{4.40}$$

Equivalently, the point $(\tilde{a}(\lambda_o), \tilde{\Omega}(\lambda_o))$, defined in (4.27), lies on a characteristic curve. In fact, (4.27) can be viewed as defining a curve $(\tilde{a}(\lambda), \tilde{\Omega}(\lambda))$ parameterized by λ. Clearly, this parametric curve incorporates the constitutive properties given by A (degree of hemitropy) and g (the axial load response function), and will henceforth be referred to as the *parametric constitutive curve*.

With this in mind, geometrically, a nontrivial solution of the linearized BVP (4.28) and (4.24) exists when a parametric constitutive curve intersects a characteristic curve. This is illustrated in Figure 4, which provides three examples of parametric constitutive curves. The nesting property of the characteristic curves guarantees that these nontrivial solutions occur in discrete modes, in analogy to the behavior of isotropic rods. Note that due to (4.27) and the constitutive assumption that $g'(\cdot) > 0$ (cf. Section 4.1), solutions for which $\Omega > 0$ (equivalently $\lambda < 1$) are *compressive*, i.e., the ends of the rod have been pushed toward each other. Conversely, solutions for which $\Omega < 0$ (equivalently $\lambda > 1$) are *tensile*, i.e., the ends of the rod have been pulled away from each other.

As is apparent in Figure 4, it is possible for a given problem to generate any finite number (including 0) or an infinite number of nontrivial solutions to the linearized BVP (4.28) and (4.24). Note that for $\lambda = 1$ (which represents the reference state of the rod, i.e. no applied end displacement), all parametric constitutive curves pass through $(a, \Omega) = (0, 0)$. As λ is varied away from $\lambda = 1$, observe that the "first" potential bifurcations occur at the intersection of the parametric curve with the characteristic curve $\mathcal{C}_1$. These solutions will be referred to as "mode 1" solutions.

We now suppose that $\lambda = \lambda_0$ is a root as in (4.40), i.e., the parametric constitutive curve intersects one of the characteristic curves, as shown in Figure 4. Then from (4.35), we may choose the nontrivial solution as follows, according to whether the characteristic curve has an odd or even subscript, respectively:

$$C_1 = \cos\frac{\omega_2^o}{2} + \frac{2}{\omega_1^o}\sin\frac{\omega_2^o}{2}, \quad C_2 = -\cos\frac{\omega_1^o}{2} - \frac{2}{\omega_2^o}\sin\frac{\omega_1^o}{2},$$
$$C_1 = \sin\frac{\omega_2^o}{2}, \quad C_2 = -\sin\frac{\omega_1^o}{2}, \tag{4.41}$$

where, in view of (4.27) and (4.30), we have

$$A(\lambda_o - 1) \;=\; \omega_1^o + \omega_2^o, \quad \lambda_o g(\lambda_o) \;=\; \omega_1^o\omega_2^o. \tag{4.42}$$

The two choices in (4.41) ensure a nonvanishing of the constants in the isotropic case $A = 0$. With the values of the constants C_1, C_2, ω_1^o, and ω_2^o given by (4.41) and (4.42), equation (4.34), and in turn (4.25) and (4.26), yield a nontrivial solution to the linearized problem (4.13) - (4.19), which we denote by

$$\boldsymbol{\xi}_o \;\equiv\; (\boldsymbol{\rho}_o, \boldsymbol{\psi}_o, (\eta_o)_\alpha). \tag{4.43}$$

It is easy to verify that $\mathcal{E}\boldsymbol{\xi}_o = \boldsymbol{\xi}_o$, i.e., $\boldsymbol{\xi}_o$ is $\mathbb{Z}_2$-invariant.

We now suppose that (4.40) and (4.43) are associated with mode 1, i.e., an intersection with $\mathcal{C}_1$, in which case we employ the first set of constants in (4.41). In order to understand the effects of hemitropy, we assume that $\tilde{a}(\lambda_o) = A(\lambda_o - 1)$ is small but nonzero. A lengthy but straightforward expansion of (4.34) and (4.25) reveals the out-of-plane deformation due to hemitropy, as illustrated in Figure 5:

$$\boldsymbol{\psi}_o(s) \;=\; \begin{bmatrix} 0 \\ -2\sin 2\pi s \end{bmatrix} + \begin{bmatrix} s\sin 2\pi s - \frac{1+\cos 2\pi s}{2\pi} \\ 0 \end{bmatrix} \tilde{a}(\lambda_o) \;+\; \dots,$$
$$\boldsymbol{\rho}_o(s) \;=\; \begin{bmatrix} \lambda\frac{1+\cos 2\pi s}{\pi} \\ 0 \end{bmatrix} + \begin{bmatrix} 0 \\ \lambda s\frac{1+\cos 2\pi s}{2\pi} \end{bmatrix} \tilde{a}(\lambda_o) \;+\; \dots. \tag{4.44}$$

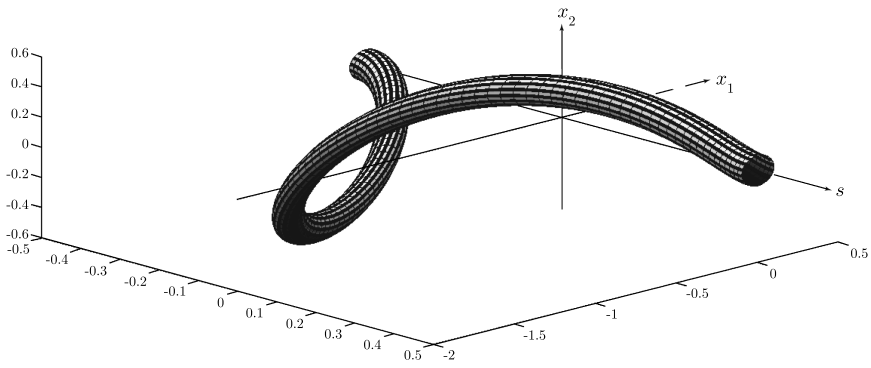

FIG. 5. The centerline $\boldsymbol{\rho}_o(s)$ corresponding to a mode 1, compressive, helical buckled configuration ($A = -37.5, g(\lambda) = 75(\lambda - 1)$).

The first terms in each expression of (4.44) correspond to the classical planar solution for an isotropic rod [15]. Observe that $A > 0$ ("right-handed" chirality; cf. [7]) implies

that $\tilde{a}(\lambda_o) < 0$, in which case $(4.44)_2$ yields a "right-handed" helical shape. Obviously $A < 0$ gives a "left-handed" helical shape, as depicted in Figure 5. Note that the reversal of chirality via the transformation $A \to -A$ corresponds to a reflection of the solution about the $\mathbf{e}_1 - \mathbf{e}_2$ and $\mathbf{e}_1 - \mathbf{e}_3$ planes.

5. Existence of local bifurcation of solutions of the fixed-fixed rod. In the previous section, we thoroughly examined the linearized solutions about straight configurations. Next we seek to prove that these linearized solutions correspond to local nontrivial solutions to the original nonlinear BVP (2.1) - (2.4), (4.3) - (4.7). To show this, we verify the standard transversality condition [3]:

$$\langle \hat{\boldsymbol{\xi}}_o, \mathbf{L}'(\lambda_o)\boldsymbol{\xi}_o \rangle \;\neq\; 0, \tag{5.1}$$

where $\mathbf{L}(\lambda)$ denotes the linearization of the operator $\mathcal{F}$ (defined in (4.8)) and is such that the linearized BVP (4.13) - (4.19) is equivalent to $\mathbf{L}(\lambda)\boldsymbol{\xi} = \mathbf{0}$; $\boldsymbol{\xi}_o = [\boldsymbol{\rho}_o, \boldsymbol{\psi}_o, (\eta_o)_\alpha]$ is a given solution (4.43), i.e. satisfying $\mathbf{L}(\lambda_o)\boldsymbol{\xi}_o = \mathbf{0}$; $\hat{\boldsymbol{\xi}}_o$ is the adjoint null solution, satisfying $\mathbf{L}^*(\lambda_o)\hat{\boldsymbol{\xi}}_o = \mathbf{0}$; and $\langle \cdot, \cdot \rangle$ is the standard L^2 inner product, i.e.,

$$\langle \boldsymbol{\xi}_1, \boldsymbol{\xi}_2 \rangle \;=\; \int_{-\frac{1}{2}}^{\frac{1}{2}} [\; \boldsymbol{\rho}_1(s) \cdot\; \boldsymbol{\rho}_2(s) \;+\; \boldsymbol{\psi}_1(s) \cdot \boldsymbol{\psi}_2(s) \;+\; (\eta_1)_\alpha (\eta_2)_\alpha \;]\; ds \quad \forall \boldsymbol{\xi}_1, \boldsymbol{\xi}_2. \tag{5.2}$$

In order to draw rigorous conclusions from (5.1), the operator $\mathbf{L}(\lambda_o)$ must have a one-dimensional null space. According to Theorem 4.2, this condition is satisfied for the fixed-fixed rod in the $\mathbb{Z}^2$ fixed-point space.

5.1. *Adjoint operator.* Given the operator $\mathbf{L}(\lambda)$, the adjoint operator $\mathbf{L}^*(\lambda)$ is determined by integration by parts, using the definition

$$\langle \mathbf{L}^*(\lambda)\hat{\boldsymbol{\xi}}, \boldsymbol{\xi} \rangle \;=\; \langle \hat{\boldsymbol{\xi}}, \mathbf{L}(\lambda)\boldsymbol{\xi} \rangle. \tag{5.3}$$

A straightforward calculation [14] shows that the adjoint BVP $\mathbf{L}^*(\lambda_o)\hat{\boldsymbol{\xi}} = \mathbf{0}$ is equivalent to the following:

$$-\hat{\eta}_\alpha'(s)\mathbf{e}_\alpha \;+\; g(\lambda)\hat{\boldsymbol{\psi}}'(s) \times \mathbf{e}_3 \;=\; \mathbf{0}, \tag{5.4}$$

$$(g'(\lambda)\hat{\boldsymbol{\rho}}''(s) \;+\; A\hat{\boldsymbol{\psi}}''(s)) \cdot \mathbf{e}_3 \;=\; 0, \tag{5.5}$$

$$\begin{aligned} &\hat{\boldsymbol{\psi}}''(s) \cdot \mathbf{e}_\alpha \mathbf{e}_\alpha \;+\; A(\lambda - 1)\hat{\boldsymbol{\psi}}' \times \mathbf{e}_3 \\ &\quad + g(\lambda)\hat{\boldsymbol{\rho}}'(s) \times \mathbf{e}_3 \;+\; \lambda \mathbf{e}_3 \times (-\hat{\eta}_\alpha \mathbf{e}_\alpha + g(\lambda)\hat{\boldsymbol{\psi}}(s) \times \mathbf{e}_3) \;=\; \mathbf{0}, \end{aligned} \tag{5.6}$$

$$(A\hat{\boldsymbol{\rho}}''(s) + B\hat{\boldsymbol{\psi}}''(s)) \cdot \mathbf{e}_3 \;=\; 0, \tag{5.7}$$

$$-(\hat{\boldsymbol{\rho}}'(s) - \lambda\hat{\boldsymbol{\psi}}(s) \times \mathbf{e}_3) \cdot \mathbf{e}_\alpha \;=\; 0, \tag{5.8}$$

$$\hat{\boldsymbol{\rho}}(\pm\frac{1}{2}) \;=\; \mathbf{0}, \tag{5.9}$$

$$\hat{\boldsymbol{\psi}}(\pm\frac{1}{2}) \;=\; \mathbf{0}. \tag{5.10}$$

By inspection, it is clear that the adjoint null solution is

$$\hat{\boldsymbol{\xi}}_o \;=\; [\hat{\boldsymbol{\rho}}, \hat{\boldsymbol{\psi}}, \hat{\eta}_\alpha] \;=\; [\boldsymbol{\rho}_o, \boldsymbol{\psi}_o, -(\eta_o)_\alpha], \tag{5.11}$$

where the components on the left side of (5.11) are as given in (4.43).

5.2. *Transversality condition.* Using the expressions (5.4) - (5.10), we now calculate the left side of (5.1). As demonstrated in [14],

$$\langle \hat{\boldsymbol{\xi}}_o,\ \mathbf{L}'(\lambda_o)\boldsymbol{\xi}_o\rangle = -(\lambda_o g'(\lambda_o) + g(\lambda_o)) \int_{-\frac{1}{2}}^{\frac{1}{2}} |\boldsymbol{\psi}_o(s)|^2 ds \ + \ A \int_{-\frac{1}{2}}^{\frac{1}{2}} (\boldsymbol{\psi}_o(s) \times \boldsymbol{\psi}_o'(s)) \cdot \mathbf{e}_3 ds. \tag{5.12}$$

In principle, this expression may vanish for particular constitutive data but is generically nonzero, as we now show. Recalling (4.27), we see that $\tilde{a}'(\lambda) = A$ and $\tilde{\Omega}'(\lambda) = -(\lambda g'(\lambda) + g(\lambda))$. Therefore, (5.12) can be rewritten as

$$\langle \hat{\boldsymbol{\xi}}_o,\ \mathbf{L}'(\lambda_o)\boldsymbol{\xi}_o\rangle \ = \ \tilde{\Omega}'(\lambda_o) \int_{-\frac{1}{2}}^{\frac{1}{2}} |\boldsymbol{\psi}_o(s)|^2 ds \ + \ \tilde{a}'(\lambda_o) \int_{-\frac{1}{2}}^{\frac{1}{2}} [\boldsymbol{\psi}_o(s) \times \boldsymbol{\psi}_o'(s)] \cdot \mathbf{e}_3 ds. \tag{5.13}$$

We now give (5.13) a geometric interpretation. As in (4.40), we substitute (4.27) and (4.29) into (4.37), yielding

$$\tilde{f}(\lambda) \ \equiv \ f(\tilde{a}(\lambda), \tilde{\Omega}(\lambda)). \tag{5.14}$$

By virtue of (4.40), we see that $\tilde{f}$ has a zero at $\lambda = \lambda_o$, and by the chain rule we have

$$\begin{aligned} \tilde{f}'(\lambda_o) \ &= \ \frac{\partial f}{\partial a}(\tilde{a}(\lambda_o), \tilde{\Omega}(\lambda_o))\tilde{a}'(\lambda_o) \ + \ \frac{\partial f}{\partial \Omega}(\tilde{a}(\lambda_o), \tilde{\Omega}(\lambda_o))\tilde{\Omega}'(\lambda_o) \\ &\equiv \ \frac{\partial f^o}{\partial a}\tilde{a}'(\lambda_o) \ + \ \frac{\partial f^o}{\partial \Omega}\tilde{\Omega}'(\lambda_o). \end{aligned} \tag{5.15}$$

Thus $\tilde{f}$ has a simple zero at λ_o when (5.15) does not vanish, and we observe the resemblence between (5.13) and (5.15). Indeed, an argument employing the shooting method [9] shows that (5.1) holds iff the left side of (5.15) does not vanish. We record this observation as

LEMMA 5.1. Given (4.40), condition (5.1) is equivalent to a transverse intersection of the parametric constitutive $(\tilde{a}(\lambda), \tilde{\Omega}(\lambda)), \lambda \in \mathbb{R}^+$, with a characteristic curve, given implicitly by (4.37), at $\lambda = \lambda_o$.

Proof. The right side of (5.15) corresponds to the inner product of the tangent to the parametric constitutive curve at the point of intersection, $(\tilde{a}'(\lambda_o), \tilde{\Omega}'(\lambda_o))$, with the normal to the characteristic curve, $(\frac{\partial f^o}{\partial a}, \frac{\partial f^o}{\partial \Omega})$. □

Finally we have

THEOREM 5.2. If (5.13) does not vanish, or equivalently if (5.15) does not vanish, then there is a smooth local "pitchfork" curve of solutions bifurcating from $(0, \lambda_o)$ of the form

$$\begin{aligned} \mathbf{x} \ \equiv \ [\mathbf{r}, \mathbf{R}, n_\alpha] \ &= \ \hat{\mathbf{x}}(\epsilon) \ = \ \mathbf{x}_o + [\epsilon\boldsymbol{\rho}_o, \epsilon\boldsymbol{\Psi}_o, \epsilon(\eta_o)_\alpha] + o(\epsilon), \\ \lambda \ &= \ \hat{\lambda}(\epsilon) \ = \ \lambda_o + o(\epsilon), \end{aligned} \tag{5.16}$$

where $\mathbf{x}_o \equiv [\lambda s \mathbf{e}_3, \mathbf{I}, (0,0)]$ denotes the straight (trivial) solution (cf. (4.11)) and $\boldsymbol{\Psi}_o$ is the unique skew tensor field such that $axial(\boldsymbol{\Psi}_o) = \boldsymbol{\psi}_o$, the latter of which is given in (4.43).

Proof. The existence of such a curve of solutions via the Implicit Function Theorem is standard; cf. [3], [10]. It remains only to show that $\hat{\lambda}'(0) = 0$ in $(5.16)_2$. Given the nonvanishing of (5.13), then in general, $\hat{\lambda}'(0)$ is proportional to the quantity

$\langle \hat{\boldsymbol{\xi}}_o, \mathcal{F}_{\mathbf{xx}}(\lambda_o, \mathbf{x}_o)[\boldsymbol{\xi}_o, \boldsymbol{\xi}_o]\rangle$ (cf. [10]), where $\mathcal{F}(\lambda, \cdot)$ is the mapping defined in (4.8) representing the nonlinear problem. From (4.9) it follows that

$$\begin{aligned}\langle \tilde{\Gamma}\hat{\boldsymbol{\xi}}_o, \mathcal{F}_{\mathbf{xx}}(\lambda_o, \mathbf{x}_o)[\Gamma\boldsymbol{\xi}_o, \Gamma\boldsymbol{\xi}_o]\rangle &= \langle \tilde{\Gamma}\hat{\boldsymbol{\xi}}_o, \tilde{\Gamma}\mathcal{F}_{\mathbf{xx}}(\lambda_o, \mathbf{x}_o)[\boldsymbol{\xi}_o, \boldsymbol{\xi}_o]\rangle \\ &= \langle \boldsymbol{\xi}_o, \mathcal{F}_{\mathbf{xx}}(\lambda_o, \mathbf{x}_o)[\boldsymbol{\xi}_o, \boldsymbol{\xi}_o]\rangle, \end{aligned} \tag{5.17}$$

for all group actions. In particular, for the rotation $\Gamma = \mathcal{Q}_\pi$ (as detailed in Table 1), we have $\mathcal{Q}_\pi \boldsymbol{\xi}_o = -\boldsymbol{\xi}_o$ and $\tilde{\mathcal{Q}}_\pi \hat{\boldsymbol{\xi}}_o = -\hat{\boldsymbol{\xi}}_o$, the substitution of which into (5.17) implies that $\langle \hat{\boldsymbol{\xi}}_o, \mathcal{F}_{\mathbf{xx}}(\lambda_o, \mathbf{x}_o)[\boldsymbol{\xi}_o, \boldsymbol{\xi}_o]\rangle = 0$. □

6. Local stability analysis of equilibria of the fixed-fixed rod. Having demonstrated the existence of locally bifurcating (nonplanar) solutions from the trivial solution, we now turn to the question of local stability. Here we adopt the standard energy criterion. An equilibrium solution is *stable* if it corresponds to a local minimum of the total potential energy in the usual C^1 topology (weak minimum); otherwise it is *unstable*.

In this section, we demonstrate that the compressed straight rod with fixed-fixed end conditions is stable for all $\lambda \in (\lambda_o^1, 1]$ and unstable for all $\lambda \in (\lambda_o^1 - \epsilon, \lambda_o^1)$, where $\epsilon > 0$ is sufficiently small and where λ_o^1 denotes the first *transversal* crossing of the parametric constitutive curve with the characteristic curve $\mathcal{C}_1$ as λ is decreased from the reference state $\lambda = 1$ (cf. Sections 4.4 and 5.2). We note, however, that this analysis is also valid whenever $\lambda_o^1 > 1$ is the first transversal crossing of the consitutive curve with $\mathcal{C}_1$, representing a nontrivial solution in tension (cf. Figure 4 with $\Omega < 0$). In this case, the trivial solution is stable for all $\lambda \in [1, \lambda_o^1)$ and unstable for all $\lambda \in (\lambda_o^1, \lambda_o^1 + \epsilon)$.

6.1. *Stability of trivial solution.* We begin with the potential energy functional

$$V(\mathbf{r}, \mathbf{R}; n_\alpha) \;=\; \int_{-\frac{1}{2}}^{\frac{1}{2}} \Big[\Upsilon(\kappa_\alpha\kappa_\alpha, \kappa_3, \nu_3) \;-\; n_\alpha \mathbf{r}' \cdot \mathbf{R}\mathbf{e}_\alpha \Big]\, ds, \tag{6.1}$$

where the components of the shear force n_α are the Lagrange multiplier fields that enforce unshearability, and Υ is defined as in (4.1). In accordance with Section 4.3, we perturb the trivial solution via (4.12). Since (4.11) represents the family of straight equilibria, we find that the first variation of the energy evaluated there vanishes, viz.,

$$\delta V_o \;=\; \frac{d}{d\epsilon}\Big[V(\lambda s\mathbf{e}_3 + \epsilon\rho(s), \exp[\epsilon\boldsymbol{\Psi}(s)]; \epsilon\eta_\alpha) \Big]_{\epsilon=0}, \tag{6.2}$$

for all smooth variations $\boldsymbol{\rho}(s)$, $\boldsymbol{\psi}(s) = axial(\boldsymbol{\Psi}(s))$, and η_α satisfying the linearized unshearability condition (4.17) and the boundary conditions (4.18) and (4.19).

Next we compute the second variation about the trivial line of solutions. A lengthy but straightforward calculation yields

$$\begin{aligned}\delta^2 V_o \;&\equiv\; \frac{d^2}{d\epsilon^2}\Big[V(\lambda s\mathbf{e}_3 + \epsilon\rho(s), \exp[\epsilon\boldsymbol{\Psi}(s)]; \epsilon\eta_\alpha) \Big]_{\epsilon=0} \\ &=\; \int_{-\frac{1}{2}}^{\frac{1}{2}} \Big[[(\psi_1')^2 + (\psi_2')^2] \;-\; A(\lambda - 1)(\psi_1'\psi_2 - \psi_1\psi_2') \;+ \lambda g(\lambda)(\psi_1^2 + \psi_2^2) \Big] \\ &\quad + \int_{-\frac{1}{2}}^{\frac{1}{2}} \Big[B(\psi_3')^2 + 2A\psi_3'\rho_3' + g'(\lambda)(\rho_3')^2 \Big] ds, \end{aligned} \tag{6.3}$$

for all admissible variations as above. Due to the assumed convexity of Υ (cf. (2.18) and (4.1)) the second of the integrals of the right side of (6.3) is nonnegative for all $\lambda \in (0,\infty)$. Indeed, the underlying 2×2 Hessian matrix is positive definite, and thus

$$\begin{aligned}\int_{-\frac{1}{2}}^{\frac{1}{2}} \Big[B(\psi_3')^2 + 2A\psi_3'\rho_3' + g'(\lambda)(\rho_3')^2\Big]ds &\geq C_\lambda \int_{-\frac{1}{2}}^{\frac{1}{2}} \Big[(\psi_3')^2 + (\rho_3')^2\Big]ds \\ &\geq C_\lambda \pi^2 \int_{-\frac{1}{2}}^{\frac{1}{2}} \Big[\psi_3^2 + \rho_3^2\Big]ds, \qquad (6.4)\end{aligned}$$

for some positive constant C_λ, where the second (Poincaré) inequality follows from the Raleigh quotient characterization of the lowest eigenvalue, subject to the linearized boundary conditions (4.18) and (4.19). Thus, it is sufficient to consider only the first of the integrals on the right side of (6.3).

As in Section 4.3, we first replace (4.17) and (4.18) with their integral equivalent (4.21). We then consider the quadratic functional

$$J(\boldsymbol{\psi},\lambda) \equiv \int_{-\frac{1}{2}}^{\frac{1}{2}} \Big[[(\psi_1')^2 + (\psi_2')^2] - A(\lambda-1)(\psi_1'\psi_2 - \psi_1\psi_2') + \lambda g(\lambda)(\psi_1^2+\psi_2^2)\Big]ds \quad (6.5)$$

subject to (4.21) and (4.24), where $\boldsymbol{\psi}(s) = \psi_\alpha(s)\mathbf{e}_\alpha$. Integrating by parts, using (4.24) shows that (6.5) has the equivalent form

$$J(\boldsymbol{\psi},\lambda) = -\int_{-\frac{1}{2}}^{\frac{1}{2}} \Big[\boldsymbol{\psi}'' + A(\lambda-1)\boldsymbol{\psi}'\times\mathbf{e}_3 - \lambda g(\lambda)\boldsymbol{\psi}\Big]\cdot\boldsymbol{\psi}\, ds, \qquad (6.6)$$

subject to (4.21) and (4.24). But J in (6.6) is also related to (4.21) and (4.23) as follows: take the dot product of (4.23) with $\boldsymbol{\psi}$ and integrate over $(-\frac{1}{2},\frac{1}{2})$. Observe that the constant term on the right side of (4.23) makes no contribution due to (4.21). This hints at a Rayleigh-quotient characterization of the minimum eigenvalue of the operator associated with (4.23) and (4.24), which we now pursue.

We first introduce the projection operator $\mathbf{P}$ defined as

$$\mathbf{P}[\boldsymbol{\psi}] = \int_{-\frac{1}{2}}^{\frac{1}{2}} \boldsymbol{\psi}(s)\, ds. \qquad (6.7)$$

Clearly $\mathbf{P}$ maps any function in $\mathcal{U} \equiv C^2([-\frac{1}{2},\frac{1}{2}],\mathbb{E}^2)$ (equipped with the usual maximum topology) into its average value. Further, $\mathbf{P}$ is both linear and continuous in both the C^0 and C^2 topologies.

Likewise, we introduce the projection

$$\mathbf{Q} = \mathbf{I} - \mathbf{P}, \qquad (6.8)$$

which maps onto the complement $\mathcal{V} \equiv \mathbf{Q}\mathcal{U}$, where $\mathbf{I}$ denotes the identity operator. Note that

$$\mathcal{V} = \{\mathbf{u}\in\mathcal{U} : \int_{-\frac{1}{2}}^{\frac{1}{2}} \mathbf{u}(s)ds = \mathbf{0}\}. \qquad (6.9)$$

Next, in view of (4.23) and (6.6), we define the operator

$$\mathbf{D}(\lambda)\boldsymbol{\psi} \equiv -[\boldsymbol{\psi}'' + A(\lambda-1)\boldsymbol{\psi}'\times\mathbf{e}_3 - \lambda g(\lambda)\boldsymbol{\psi}], \qquad (6.10)$$

and we consider the following eigenvalue problem:

$$\mathbf{D}(\lambda)\boldsymbol{\psi} \;+\; [\boldsymbol{\psi}(\frac{1}{2}) - \boldsymbol{\psi}(-\frac{1}{2})] \;=\; \sigma\boldsymbol{\psi}, \tag{6.11}$$

for all $\boldsymbol{\psi} \in \mathcal{V}$, subject to (4.24). A direct calculation from (6.7) and (6.10) shows that for all such $\boldsymbol{\psi}$,

$$\mathbf{PD}(\lambda)\boldsymbol{\psi} \;=\; -[\boldsymbol{\psi}(\frac{1}{2}) - \boldsymbol{\psi}(-\frac{1}{2})]. \tag{6.12}$$

Next we define the linear operator $\mathbf{H}$ via its action

$$\mathbf{H}(\lambda)\boldsymbol{\psi} \;\equiv\; \mathbf{QD}(\lambda)\boldsymbol{\psi}, \tag{6.13}$$

for all $\boldsymbol{\psi} \in \mathcal{V}$, and the associated eigenvalue problem

$$\mathbf{H}(\lambda)\boldsymbol{\psi} \;=\; \sigma\boldsymbol{\psi}. \tag{6.14}$$

Observe that (6.11) is equivalent to (6.12) and (6.14). Note further that (6.12) is independent of the eigenvalue σ, while (6.14) contains no inhomogeneous boundary terms.

By virtue of (6.6) and (4.21), it follows that

$$J(\boldsymbol{\psi}, \lambda) \;=\; \int_{-\frac{1}{2}}^{\frac{1}{2}} \boldsymbol{\psi}(s) \cdot \mathbf{H}(\lambda)\boldsymbol{\psi}(s)\; ds, \tag{6.15}$$

and it is easy to demonstrate that $\mathbf{H}$ is formally self-adjoint. Therefore, the minimization of the quadratic functional (6.15) on the appropriate unit sphere (cf. [12]) yields the following characterization of the minimum eigenvalue of (6.11), denoted by σ_1:

$$J(\boldsymbol{\psi}, \lambda) \;\geq\; \sigma_1 \int_{-\frac{1}{2}}^{\frac{1}{2}} \boldsymbol{\psi}(s) \cdot \boldsymbol{\psi}(s)\; ds, \tag{6.16}$$

for all $\boldsymbol{\psi} \in \mathcal{V}$ satisfying (4.24). With this background, we now demonstrate that the trivial solution is stable "up until" the first critical value λ_o^1 and that the stability changes as λ crosses λ_o^1.

THEOREM 6.1. The straight (trivial) state, characterized by (4.11), is stable for all $\lambda \in (\lambda_o^1, 1]$ (or $\lambda \in [1, \lambda_o^1)$).

Proof. Consider the eigenvalue problem (6.11), or equivalently (6.12) and (6.14) on $\mathcal{V}$, which can be written as

$$\boldsymbol{\psi}'' \;+\; A(\lambda - 1)\boldsymbol{\psi}' \times \mathbf{e}_3 \;+\; [\sigma - \lambda g(\lambda)]\boldsymbol{\psi} \;=\; \boldsymbol{\psi}(\frac{1}{2}) - \boldsymbol{\psi}(-\frac{1}{2}), \tag{6.17}$$

subject to (4.21) and (4.24). But (6.17) can be solved by the same reasoning as in Section 4. In analogy with (4.27), we define

$$a \;=\; A(\lambda - 1), \qquad \hat{\Omega} \;=\; \sigma - \lambda g(\lambda). \tag{6.18}$$

Then (6.17) has the same form as (4.28), which has nontrivial solutions iff $(a, \hat{\Omega})$ belongs to one of the characteristic curves $\mathcal{C}_i$, $i = 1, 2, 3, ...$; cf. Figure 4. Thus for any fixed $\lambda \in (0, \infty)$, we obtain a sequence of eigenvalues σ_i, $i = 1, 2, 3, ...$, in correspondence with the vertical line $a = A(\lambda - 1)$ with the characteristic curves. In particular, for any $\lambda \in (\lambda_o^1, 1]$, the least eigenvalue satisfies $\sigma_1 = \hat{\Omega}_1(\lambda) + \lambda g(\lambda) > 0$, where $(A(\lambda - 1), \hat{\Omega}_1(\lambda))$

denotes the point of intersection of the aforementioned vertical line with the characteristic curve $\mathcal{C}_1$. The claim now follows directly from (6.16). □

THEOREM 6.2. The straight (trivial) state, characterized by (4.11), is unstable for all $\lambda \in (\lambda_o^1 - \epsilon, \lambda_o^1)$ (or $\lambda \in (\lambda_o^1, \lambda_o^1 + \epsilon)$) for $\epsilon > 0$ sufficiently small.

Proof. As in Section 4.4, we restrict (6.14) to the $\mathbb{Z}^2$ fixed point space; cf. (4.32):

$$\mathcal{V}_{\mathbb{Z}^2} \;=\; \{\boldsymbol{\psi} \in \mathcal{V} : \mathbf{E}\boldsymbol{\psi}(-s) = \boldsymbol{\psi}(s) \text{ on } (-\frac{1}{2}, \frac{1}{2})\}. \tag{6.19}$$

In view of the equivalence of (6.11) and (6.14), the same argument used in the proof of Theorem 6.1 shows that $\mathbf{H}(\lambda_o^1)$ has a simple zero eigenvalue with accompanying nullvector $\boldsymbol{\psi}_o$. We further assume that $\boldsymbol{\psi}_o$ is normalized such that $\langle \boldsymbol{\psi}_o, \boldsymbol{\psi}_o \rangle = 1$. Then, dotting each side of (6.14) with $\boldsymbol{\psi}_o$, integrating over $(-\frac{1}{2}, \frac{1}{2})$, and differentiating with respect to λ, we have

$$\begin{aligned} \sigma'(\lambda_o^1) &= \int_{-\frac{1}{2}}^{\frac{1}{2}} \boldsymbol{\psi}_o(s) \cdot \mathbf{H}'(\lambda_o^1)\boldsymbol{\psi}(s)\, ds \\ &= A \int_{-\frac{1}{2}}^{\frac{1}{2}} (\boldsymbol{\psi}_o(s) \times \boldsymbol{\psi}_o'(s)) \cdot \mathbf{e}_3 \, ds \;\; - (\lambda_o g'(\lambda_o) + g(\lambda_o)) \int_{-\frac{1}{2}}^{\frac{1}{2}} |\boldsymbol{\psi}_o(s)|^2 ds. \end{aligned} \tag{6.20}$$

Note that the right side of (6.20) is equivalent to the right side of (5.12).

The local continuity of the simple eigenvalue $\sigma(\lambda)$ for $|\lambda - \lambda_o^1| < \epsilon$ is readily established via the Implicit Function Theorem [10], and the transversality condition (5.12) implies that the zero eigenvalue changes sign as λ "crosses" λ_o^1. Thus we have

$$\begin{aligned} J(\boldsymbol{\psi}_o, \lambda) &= \int_{-\frac{1}{2}}^{\frac{1}{2}} \boldsymbol{\psi}_o(s) \cdot \mathbf{H}(\lambda)\boldsymbol{\psi}_o(s)\, ds \\ &= \sigma(\lambda) \\ &< 0 \quad \text{for all } \lambda \in (\lambda_o^1 - \epsilon, \lambda_o^1). \end{aligned} \tag{6.21}$$

Finally, recalling (6.3) and (6.6), we choose $\psi_\alpha(s)\mathbf{e}_\alpha = \boldsymbol{\psi}_o(s)$ with $\psi_3(s) = \rho_3(s) = 0$, and thus conclude that $\delta^2 V_o < 0$ for all $\lambda \in (\lambda_o^1 - \epsilon, \lambda_o^1)$. □

6.2. *Local stability of mode* 1 *bifurcating branches.* Having established the change of stability of the trivial solution at a mode 1 bifurcation point $\lambda = \lambda_o^1$, we now turn to the question of the local orbital stability of mode 1 bifurcating branches. We use "orbital" here to signify that, due to (4.9), all nontrivial solutions belong to $SO(2)$-generated orbits of solutions. Given the flip symmetry of this problem, the bifurcating branches form "pitchforks"; cf. (5.16). For bifurcation points λ_o at compressive (tensile) states, λ decreases (increases) across λ_o as the trivial solution passes from stable to unstable. By virtue of standard exchange-of-stability results, e.g., [10], we find that the compressive (tensile) bifurcating branch is orbitally, locally stable if the pitchfork opens to the left (right) along the positive λ axis. In both cases this leads to the condition

$$\langle \hat{\boldsymbol{\xi}}_o^1, \mathcal{F}_{\mathbf{xxx}}(\lambda_o^1, \mathbf{x}_o^1)[\boldsymbol{\xi}_o^1, \boldsymbol{\xi}_o^1, \boldsymbol{\xi}_o^1] \rangle \;<\; 0, \tag{6.22}$$

where $\mathbf{x}_o^1 = [\mathbf{r}_o^1, \mathbf{R}_o^1, (n_o^1)_\alpha] = [\lambda s \mathbf{e}_3, \mathbf{I}, (0,0)]$, $\boldsymbol{\xi}_o^1 = [\boldsymbol{\rho}_o^1, \boldsymbol{\psi}_o^1, (\eta_o^1)_\alpha]$, and $\hat{\boldsymbol{\xi}}_o^1 = [\boldsymbol{\rho}_o^1, \boldsymbol{\psi}_o^1, -(\eta_o^1)_\alpha]$ are the trivial solution, linearized solution (cf. (4.43)), and adjoint linearized solution (cf. (5.11)) at $\lambda = \lambda_o^1$, respectively.

A very long but straightforward calculation reveals that

$$\begin{aligned}
&\langle \hat{\boldsymbol{\xi}}_o^1, \mathcal{F}_{\mathbf{xxx}}(\lambda_o^1, \mathbf{x}_o^1)[\boldsymbol{\xi}_o^1, \boldsymbol{\xi}_o^1, \boldsymbol{\xi}_o^1] \rangle \\
&\quad = \int_{-\frac{1}{2}}^{\frac{1}{2}} \Big[(-3\lambda^2 g'(\lambda) - 5\lambda g(\lambda)) |\boldsymbol{\psi}_o^1(s)|^4 + (7+3B)[(\boldsymbol{\psi}_o^1(s) \times (\boldsymbol{\psi}_o^1)'(s)) \cdot \mathbf{e}_3]^2 \\
&\qquad + \ A(\lambda - 6) |\boldsymbol{\psi}_o^1(s)|^2 (\boldsymbol{\psi}_o^1(s) \times (\boldsymbol{\psi}_o^1)'(s)) \cdot \mathbf{e}_3 - 16 (\psi_1')_o^1(\tfrac{1}{2}) |\boldsymbol{\psi}_o^1(s)|^2 (\psi_1)_o^1(s) \Big] ds \ .
\end{aligned} \tag{6.23}$$

Observe that the right side of (6.23) depends on the specific form of the eigenfunction $\boldsymbol{\psi}_o^1(s)$ and upon all of the principal constitutive data: the response function $g(\cdot)$, the hemitropic modulus A, and twisting modulus B (and implicitly on the bending modulus $C = 1$; cf. Section 4.1). It is difficult to verify (6.22) at the level of generality of (6.23). Nonetheless, it can be shown that the expression (6.23) is invariant under the transformation $A \to -A$, which is reassuring. It's also worth noting that in the case of isotropy, $A = 0$, where all but the first term in the integrand of (6.23) vanish, by virtue of (4.44). In particular, we find for normalized $\boldsymbol{\psi}_o^1$,

$$\langle \hat{\boldsymbol{\xi}}_o^1, \mathcal{F}_{\mathbf{xxx}}(\lambda_o^1, \mathbf{x}_o^1)[\boldsymbol{\xi}_o^1, \boldsymbol{\xi}_o^1, \boldsymbol{\xi}_o^1] \rangle \ = \ -\frac{3}{2}(3\lambda^2 g'(\lambda) + 5\lambda g(\lambda)) \ + \ O(A^2). \tag{6.24}$$

In view of (6.22), we conclude:

THEOREM 6.3. For A^2 sufficiently small, the local nontrivial branch of solutions (5.16), associated with the a mode 1 bifurcation point at $\lambda = \lambda_o$, is orbitally stable if

$$g'(\lambda) \quad > \quad \frac{-5g(\lambda)}{3\lambda} \quad \text{for all } \lambda > 0. \tag{6.25}$$

7. Conclusions. We present a description of unshearable, hemitropic rods in terms of the Cosserat theory. Our basic model indicates what is commonly observed, viz., that such rods have an intrinsic coupling between extension and twist. This is analogous to the Poisson effect in which axial and transverse deformation are coupled.

We first consider unshearable hemitropic rods under fixed-free end conditions and subject to dead axial load. We demonstrate the striking result that despite the presence of hemitropy, all solutions are planar. A physical explanation is that under axial thrust, although the rod twists, it does not develop internal axial torque.

We next consider the behavior of unshearable hemitropic rods under fixed-fixed end conditions and subject to prescribed axial displacement. In this case an internal axial torque develops in the straight loaded state, leading to an initial, nonplanar buckled state (cf. Figure 5). This is in stark contrast to the initial, planar buckling of isotropic rods under end thrust. By virtue of (4.44), the magnitude of the out-of-plane component of the displacement, to first order, is proportional to the hemitropic modulus A. In particular, the linearized solutions reduce to those of the isotropic rod in the limit as $A \to 0$.

In analogy to the isotropic case, the bifurcating solutions for the hemitropic case occur in discrete modes. Indeed, as illustrated in Figure 4, a set of nested, nonintersecting characteristic curves specify the general combinations of axial thrust and hemitropic modulus that must be satisfied by any nontrivial solution within the constitutive class that we consider. We further prove the genericity of the existence of bifurcation for rods of our constitutive class, and in particular, present an equivalent geometric condition that is graphically clear: if the parametrically defined constitutive data curve intersects a characteristic curve nontangentially, then nontrivial solutions exist at that point (cf. Figure 4). We infer from Figure 4 that the presence of hemitropy ($A \neq 0$) lowers the first compressive buckling load compared to the isotropic case ($A = 0$). We also note that while the determination of bifurcation is critically dependent on the hemitropic modulus A, it is independent of the twisting modulus B (cf. (5.13)).

In addition to the nonplanarity, the solutions of the fixed-fixed hemitropic rod differ from the fixed-fixed isotropic rod in another important way. Nontrivial solutions for isotropic rods are necessarily compressive; the impossibility of such nontrivial tensile solutions can be inferred from Figure 4 (with $a = 0$). However, it is possible to attain both compressive and tensile nontrivial solutions for hemitropic rods, as also illustrated in Figure 4. This is similar to the instability of highly twisted isotropic rods in tension; cf. [11].

Our results further provide local stability properties of equilibria of the fixed-fixed hemitropic rod. The trivial solution is stable for all values of prescribed end displacement below a critical threshhold. We further provide a calculation for the determination of the orbital stability of mode 1 bifurcating branches that is, in general, dependent on the given constitutive data. We note that while the stability of the trivial solution is independent of the twisting modulus B (cf. Section 6.1), the stability of the bifurcating branches generally depends on B; cf. (6.23).

The specific form of the stored energy function (4.1) employed in Sections 4-6 is for convenience only, i.e., we could easily obtain the same results for a more general class of convex hemitropic stored energy functions. Finally we mention that, with the local analysis in hand, a detailed global bifurcation analysis of the problem (4.3) - (4.7) can be carried out via methods similar to those employed in [1]. This will be pursued in a future work.

Acknowledgements. We thank Prashant Mehta, Rob Manning and Ajeet Kumar for useful discussions at various stages of this work. The work of Timothy J. Healey presented herewith was supported in part by the National Science Foundation through grants DMS-0072514 and DMS 1007380. The work of Christopher M. Papadopoulos presented herewith was supported in part by a Graduate Research Fellowship from the National Science Foundation. The authors gratefully acknowledge this support.

References

[1] S.S. Antman and C.S Kenney, Large buckled states of nonlinearly elastic rods under torsion, thrust and gravity, *Arch. Rat. Mech Anal.* 76, 289-338 (1981). MR628172 (82k:73043)

[2] S.S. Antman, *The Nonlinear Problems of Elasticity*, 2nd Ed., Springer-Verlag, New York, 2005. MR2132247 (2006e:74001)
[3] M.G. Crandall and P. H. Rabinowitz, Bifurcation from simple eigenvalues, *J. Funct. Anal.* 8, 321-340 (1971). MR0288640 (44:5836)
[4] G. Costello, *The Theory of Wire Rope*, Springer-Verlag, New York, 2007. MR1101811 (92c:73104)
[5] L. Euler, *Additamentum I de curvis elasticis, methodus invieniendi lineas curvas maximi minimivi proprietate gaudentes*, Bousquent, Lausanne, in *Opera Omnia* I, Vol. 24, 234-297 (1744).
[6] T.J. Healey, Global bifurcation and continuation in the presence of symmetry with an application to solid mechanics, *SIAM J. Math. Anal.*, 19, 824-839 (1988). MR946645 (89k:58058)
[7] T.J. Healey, Material symmetry and chirality in nonlinearly elastic rods, *Math. Mech. Solids* 7, 405-420 (2002). MR1921465 (2003g:74053)
[8] T.J. Healey, A rigorous derivation of hemitropy in nonlinearly elastic rods, *DCDS-B* 16, 265-282 (2011). MR2799551
[9] J.B. Keller, Bifurcation theory for ordinary differential equations, in *Bifurcation Theory and Nonlinear Eigenvalue Problems*, Eds. J.B. Keller & S.S. Antman, W.A. Benjamin, Inc., New York, 1969.
[10] H. Kielheofer, *Bifurcation Theory: An Introduction with Applications to PDE's*, Springer-Verlag, New York, 2004. MR2004250 (2004i:47133)
[11] A.E.H. Love, *A Treatise on the Mathematical Theory of Elasticity*, 4th Ed, Cambridge University Press, Cambridge, 1927.
[12] R.S. Manning, K.A. Rogers, and J.H. Maddocks, Isoperimetric conjugate points with application to the stability of DNA minicircles, *Proc. Roy. Soc. Lond. A* 454, 3047-3074 (1998). MR1664277 (99j:49032)
[13] J.F. Marco, Stretching must twist DNA, *Europhys. Lett.* 38, 183-188 (1997). MR1446825 (98b:92004)
[14] C.M. Papadopoulos, *Buckled States of Compressed Hemitropic Rods*, Ph.D. Dissertation, Cornell University, Ithaca, NY, 1999.
[15] S.P. Timoshenko and J.M. Gere, *Theory of Elastic Stability*, 2nd Ed., McGraw-Hill, New York, 1951. MR0134026 (24:B80)
[16] J.L. Synge and B.A. Griffith, *Principles of Mechanics*, 3rd Ed., McGraw-Hill, New York, 1959. MR0106562 (21:5293)